BILINGUAL
PUBLISHING CO.
Pioneer of Global Academics Since 1984

Journal of Architectural Environment & Structural Engineering Research

Volume 5 • Issue 3 • July 2022 ISSN 2630-5232(Online)

Volume 5 Issue 3 · July 2022 · ISSN 2630-5232(Online)

Journal of Architectural Environment &Structural Engineering Research

BILINGUAL
PUBLISHING CO.
Pioneer of Global Academics Since 1984

BILINGUAL PUBLISHING CO.
Pioneer of Global Academics Since 1984

Volume 5 | Issue 3 | July 2022 | Page1-51

Journal of Architectural Environment & Structural Engineering Research

Contents

Retraction notice

Articles

Journal of Architectural Environment & Structural Engineering Research
https://ojs.bilpublishing.com/index.php/jaeser

RETRACTION NOTICE

RETRACTED: A Comparative Study between Pseudo-static and Dynamic Analyses of Keddara Dam

Manish Sharma*

Department of Civil Engineering, Faculty of Engineering and Technology, Jamia Millia Islamia, New Delhi, 110025, India

This article has been retracted. The above authors were identified and corrected for alleged falsification of research, data fabrication and other misconduct.

JAESER editorial team takes the issue of integrity seriously and does not allow any tampering with scientific articles. We apologize for any inconvenience this retraction may cause to JAESER readers.

Refers to:

We, the Editors and Publisher of *Journal of Architectural Environment & Structural Engineering Research*, have retracted the following article:

Article title: A Comparative Study between Pseudo-static and Dynamic Analyses of Keddara Dam

Author: Manish Sharma

Journal: Journal of Architectural Environment & Structural Engineering Research

Bibiliometrics: Volume 5, Issue 2, pages 16-24.

DOI: https://doi.org/10.30564/jaeser.v5i2.4675

**Corresponding Author:*
Manish Sharma,
Department of Civil Engineering, Faculty of Engineering and Technology, Jamia Millia Islamia, New Delhi, 110025, India

DOI: https://doi.org/10.30564/jaeser.v5i3.4880

BILINGUAL PUBLISHING CO.
Pioneer of Global Academics Since 1984

Journal of Architectural Environment & Structural Engineering Research
https://ojs.bilpublishing.com/index.php/jaeser

ARTICLE

Analysis and Assessment of Selected Iranian Contemporary Buildings by Well-Building Criteria

Shahram Salimi Sotoudeh* **Shadi Tabarsi**

Department of Architecture, Faculty of Engineering, Shoushtar Branch, Islamic Azad University, Shoushtar, Iran

ARTICLE INFO

Article history
Received: 6 July 2022
Revised: 18 August 2022
Accepted: 26 August 2022
Published Online: 31 August 2022

Keywords:
Well AP
Sustainability
Beauty design
LEED AP

ABSTRACT

Aims: Pandemics have brought about new conditions to today's life and designing well-buildings is now a priority. However, having a peek at the prior studies reveals that the most important issue in this area is the disharmony among the different elements of well-buildings. The main objective of this article is addressing the complexities of studying all requirements of such buildings. **Methods**: The main means of undertaking this research are case studies, indeed. First, the ten selected cases will be analyzed by means of the theoretical framework of this research. Then, the results shall be discussed based upon the fundamental design theory, and finally practical resolutions will be suggested. **Findings**: Seven fundamental elements including Air, Water, Nourishment, Light, Fitness, Comfort, and Mind are all simply achievable separately; however, an analysis of the case studies has revealed that gathering them all together would not be an easy task to undertake. **Conclusions**: This study has revealed that the problem of mingling and uniting these seven principal elements is serious and it is rather difficult to put together such elements, simultaneously. Finally, design approach to the very principles is the most important suggestion of this study since it is clear that in the world of architecture, unification is of high importance. Therefore, the secret to the beauty of healthy architecture is the unification of design of all the elements.

1. Introduction

The factors that contribute to a healthy building are numerous and can be explored from several angles. Many requirements must be met in order for a building to be considered healthy. Sound design and construction are required for each building's technical functioning and mechanical stability, as well as the basic safety of its occupants. However, this is insufficient to ensure the occupants' indoor environmental quality (IEQ). A variety of other factors have an impact on the occupants' well-being, either directly or indirectly. Heating, ventilation, and air conditioning are examples of such factors, as are occupant activities such as the use of office equipment or household

*Corresponding Author:
Shahram Salimi Sotoudeh,
Department of Architecture, Faculty of Engineering, Shoushtar Branch, Islamic Azad University, Shoushtar, Iran;
Email: salimisotoudeh.sh@gmail.com

DOI: https://doi.org/10.30564/jaeser.v5i3.4871

activities such as cooking, cleaning, or applying pesticides [1].

Current green building criteria are superficial and insufficient for specifying materials and developing ventilation systems to create a healthy indoor atmosphere, i.e. a "healthy building" by design. Public perception, cultural preferences, litigation trends, current codes and regulations, as well as the rapid introduction of new building materials and commercial products, as well as the prevalent design-build practices, all pose challenges to systems integration in the design, construction, and operation phases of modern buildings. We are on the threshold of a paradigm change in the way we think about ventilation design. Previously, the thermal qualities of the air inside a zone governed heating, ventilation, and air-conditioning parameters. The use of occupant-specific and highly sensitive systems will become the standard in the future [2].

The significant subjective changes of indoor discuss and the dynamic increment within the outright number of toxins, combined with the logical mindfulness of the well-being impacts determining from investing more than 90% of one's time interior restricted spaces, have increased the consideration onto the requirements of well-being, cleanliness, and the wellbeing of clients. This logical consideration has delivered considers and investigations valuable for evidence-based experiences into building execution [4].

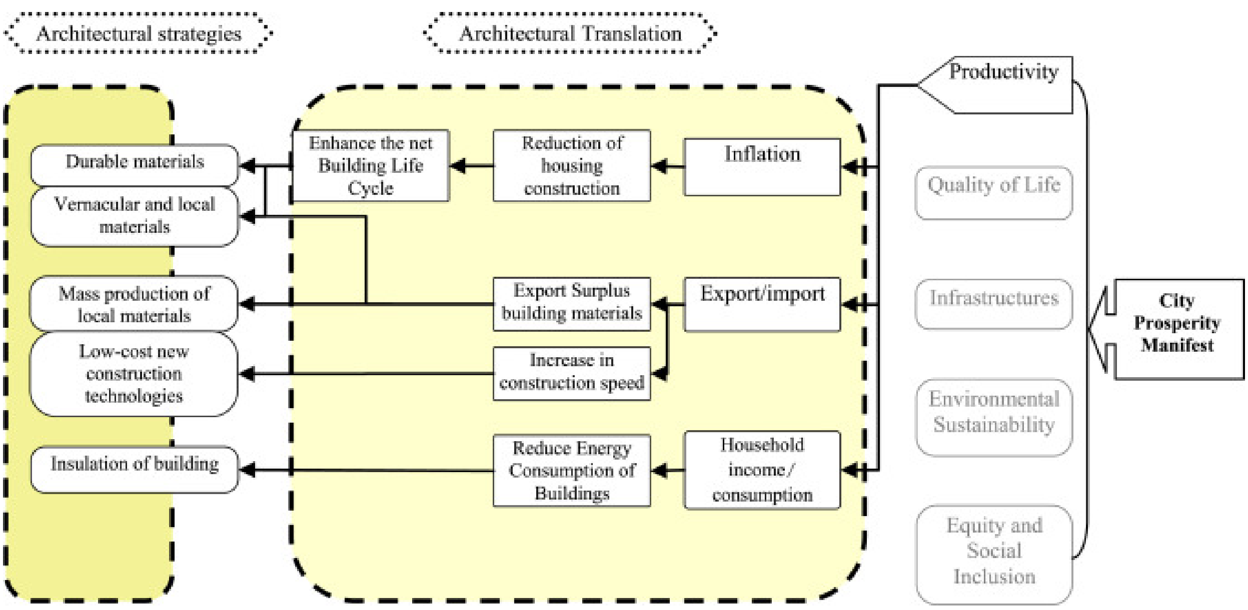

Figure 1. Workflow from idea to design [3]

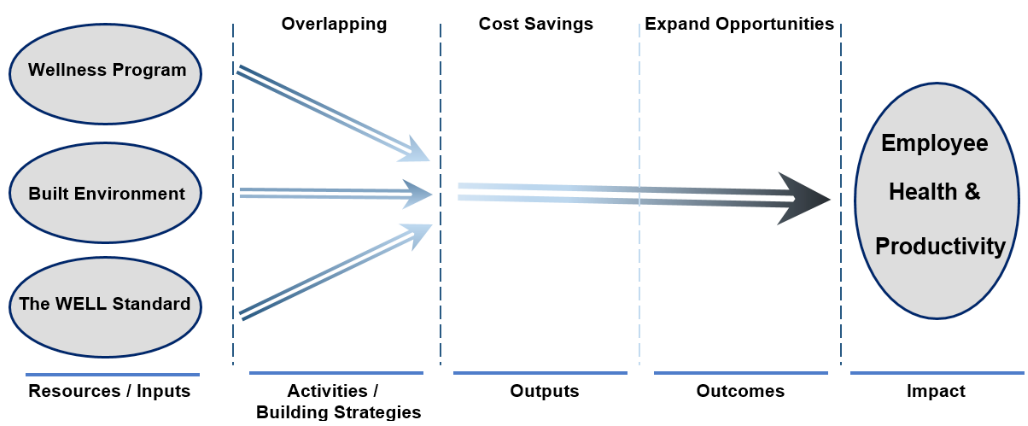

Figure 2. A framework to incorporate wellness programs, built environment, and the well building standard

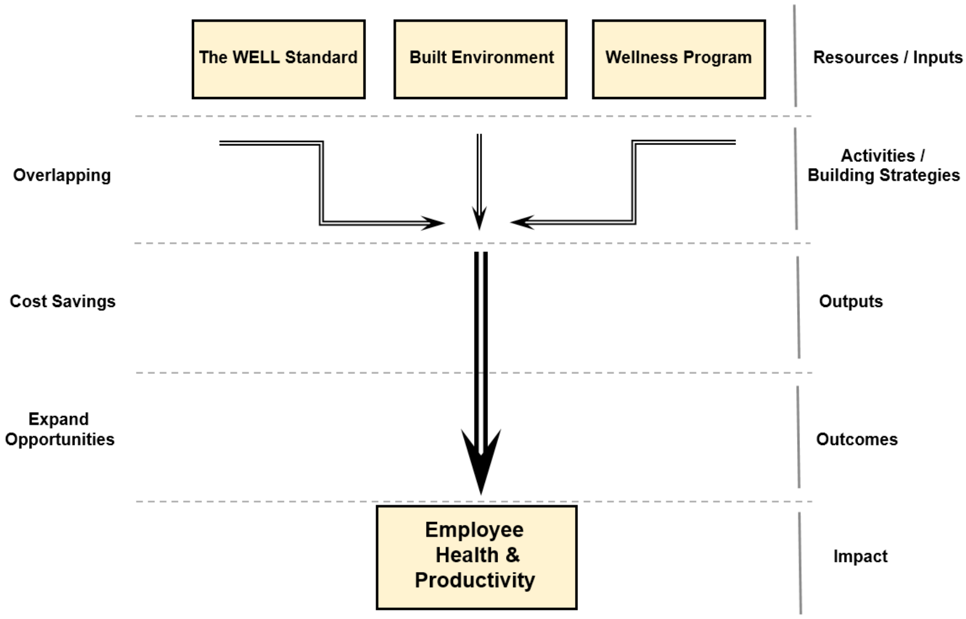

Figure 3. The well-building framework promotes sustainability and efficiency

Among the main pollutants in the indoor environment, Volatile Organic Compounds (VOCs) play a central role, and the use of box-models using the mass balance approach and Computational Fluid Dynamics (CFD) models are now consolidated to study their concentrations in an indoor environment [4].

2. Literature Review

Since 2013, the International WELL Building Institute (IWBI) has commenced its measures in progressing global culture of health through better buildings. It has, moreover, cooperated with corporations which have activities in sustainable architecture and has been approved by them.

"WELL Building Standards" program was the first environmental assessment program in the world to focus on well-being and human health within the administrative building by means of interior designing. Enhancing the physical and psychological health of the human being is done by improving the quality of indoor environment of the building, and it is necessary to resort the "WELL Building Standards" program and using its standards in the interior design [5].

The literature highlights the Rose Bowl at Leeds Beckett University is an iconic building designed to BREEAM Excellent. The experience of staff and pupils in classrooms, offices and lecture theatres was proving to be less than excellent. In order to assess and quantify the different parameters that characterize the Indoor Environment (IE) an Australian Government developed tool, NABERS Indoor Environment was used to evaluate the Rose Bowl. The results of the assessment revealed that the IE in the Rose Bowl less than optimal for staff and student health and weelbeing. There were shortcomings in thermal, acoustic and lighting comfort. In addition, indoor air quality (IAQ) was also not optimal for people. The most significant finding was elevated levels of formaldehyde, which can have significant effects on occupant health [6]. In 2021, California made historic changes to its early learning system [7] that refers to understanding the value of health more than ever.

Rani et al. (2022) studied factors affecting workplace well-being and building construction projects in order to explain healthy concepts of design. Well-being encompasses both physical and mental health, leading to more comprehensive approaches to illness prevention and health promotion [8]. Lower levels of happiness have been linked to an increased risk of disease, illness, and injury, as well as impaired immune function, delayed recovery, and shorter lifespans [9-13]. Asniza Hamimi Abdul Tharim et al. (2022) in "the determinant factors of biophilic design strategies and occupants' psychological performance in office building" emphasized on the role of the design strategies. Urbanization can result in the changing of climate change, global warming, threatens biodiversity, and decrease access to the natural environment. Hence the current lifestyle and urban living make people distance themselves from the natural world, especially during working hours. Therefore, biophilic design strategies function to eradicate the void between modern design, urbanization, and human needs [14].

RazlinMansor and Low Sheau-Ting (2022) in "a measurement model of occupant well-being for Malaysian office building" highlights [15]:

- Indoor environment impacted occupant well-being in an office building.
- AHP methodology was adopted to assign the priority weight.
- The priority weight of the occupant well-being criteria and associated indoor environment parameters for Malaysian office building were determined.
- Occupant health has the highest priority, followed by occupant comfort, occupant safety and occupant adaptation.
- A measurement model of occupant well-being for Malaysian office building was developed.

The literature highlights Human well-being is the responsibility of architects and interior designers. According to their professional position, they must examine many aspects of the surrounding context and the users' environmental parameters [16,17]. The literature emphasizes on the adoption status of sustainable energy technologies [18,19] by controlling the sick building syndrome (SBS). At present, with more and more attention paid to the impact of buildings on the health and well-being of occupants, sick building syndrome (SBS) has become a global concern. Since the introduction of SBS by the World Health Organization (WHO) in 1983, thousands of research literature have been published in this field [19]. Houser et al. (2022) in a method and tool to determine the colorimetric and photobiological properties of light transmitted through glass and other optical materials, showed that synthesis of colorimetric and biological quantities that can be derived from spectral data. It is to be understood that energy and environment have a lot to do with healthy concept and well-building [21]. Securing well-being and building resilience in response to shocks are often viewed as key goals of sustainable development. The literature emphasizes on the role of design in health and well-being [22-27]. Redesign of ZEB Lab building at NTNU was a sample of prioritising passive climate control which shifted toward healthy concept of well-building [28]. The well Building Standard is the first of its kind to focus on the health and wellness of building occupants. It's a dynamic rating system between design and construction with evidence-based health and wellness interventions. It's a holistic design approach addressing seven concepts: air, water, nourishment, light, fitness, comfort, and mind. Within these concepts are 100 "features" intended to address specific aspects of occupant health, comfort, and knowledge. To model these concepts and features, I will be using my Spring 2022 interior design studio project to exemplify the importance and benefits of the well Building Standard in workplace design [29]. The well concepts that support office building occupants' health, well-being, and productivity in a developing country [30]. In the last three decades, many green and sustainable building standards have been established. These standards, however, focus on delivering environment-conscious and energy-saving buildings rather than supporting occupants' health, well-being, and productivity [30]. Recently, the evaluation of well COVID-19 certificate [31] resulted in a promising horizon for meeting the health of the occupants.

The Well-Building Standard is organized into seven categories of wellness called Concepts: Air, Water, Nourishment, Light, Fitness, Comfort and Mind for which specific architectural design standards are mandatory. According to these categories, the International WELL Building Institute (IWBI) issues a certification which enhances the prestige of a brand; like what takes place with ISO certifications. The certification can be issued for construction projects which are planned, in progress or completed and it indicates that these projects have prioritize health issues of customers, employees and employers. This will lead in a uniform attitude.

The certification is issued in three classifications: Silver, Golden and Platinum. For Silver, all prerequisites are required where for Golden all the prerequisites and 40 percent of optimization indicators are essential. Platinum indicates that all the prerequisites plus 80 percent of optimization indicators have been complied with. In order to apply for certification five steps should be taken:

- Registration
- Documents Submission (Required Documents: Annotated Documents, Letters of Assurance (LOAs), General Documents)
- Performance Verification
- Certification Issuance
- Annual Renewal

3. Methodology

The research methodology is based on a comprehensive approach to architectural design process. The research is based on descriptive-analytical methodology. It is to elaborate a discussion in order to find out what the concept of well-building are. The number of the case studies in descriptive and analytical research methodology depends on the quality and quantity of the research. Therefore, the quality and quantity of research dictate the number of cases that are needed in the research [32,33]. The cases are selected by purposive sampling (non-probability sampling) which is also known as judgment, selective or subjective sampling technique. When the researcher relies on his or her own expertise in the field and his or her judgment, "purposive sampling" (with focused sampling orientation) [34,35] is the best choice for choosing members of the population for studying.

In order to explain and described the method more clearly, it is necessary to have a deep look and further explaination about expert-based analysis in combination with focus group discussion (FGD) technic. The samples of the research was a kind of purposive sampling; therefore, a group of experts including two experienced architects, three related experts (a bank manager, a health assessment expert and a socio-cultural scholar) gathered to analyze the case studies in depth and more precisely. The results are enriched by the group in a close collaboration.

4. Case Study

Tehran is the most leading city in the field of architecture in Iran. Iran is a young country in using electronic banking and it has a long way to reach an acceptable and now people have to go to the branches physically, thus, banks are well case studies with having many branches, employees and customers. Consequently, all the case studies are selected from among Tehran banks.

The research team knows the most important case studies in contemporary architecture of Iran. Therefore, ten different cases have been studied and analyzed:

- Tehran, Pasargad Bank, Pamenar Branch
  (Branch No. 389,Corner of Marvi, Pamenar st., Panzdah-e-Khordad st., Tehran, 1116965915, IRAN)
- Tehran, Melli Bank, Daneshgah Tehran Branch
  (No. 1168, Between University and Aboureyhan st., Enghelab st., Tehran, 1315693681, IRAN)
- Tehran, Melli Bank, Fakhr Razi Branch
  (No. 1228, In Front of Tehran University, After Fakhr-e-Razi st., Enghelab st., Tehran, 1314754361, IRAN)
- Tehran, Maskan Bank, Sattar khan Branch
  (No. 34, Lower of Habibollah st., Sattar khan st., Tehran, 1455864886, IRAN)
- Tehran, Ayandeh Bank, Ekbatan Town Branch
  (No. 20, Corner of Tusi Alley, Nafisi St., Phase 1, Ekbatan Town., Tehran, 1393864514, IRAN)
- Tehran, Saderat Bank, 17 Shahrivar Branch
  (No. 116, Above of Mansour Cross, South Hefdah Shahrivar st., Tehran, IRAN)
- Tehran, Saman Bank, Nafisi St. Branch
  (No. 59, In Front of Mokhaberat, Nafisi St., Phase 1, Ekbatan Town., Tehran, 1393844181, IRAN)
- Tehran, Keshavarzi Bank, Habibollah Branch
  (Branch No. 29000, Corner of Habibollah Junc., Sattar khan st., Tehran, , IRAN)
- Tehran, Mellat Bank, Valiasr-Beheshti Branch
  (No. 371, Corner of Beheshti St., Valiasr St., Tehran, 1595783115, IRAN)
- Tehran, Sepah Bank, Tehran Villa Branch
  (No. 327, Corner of Niyayesh St., In Front of Habibollah St., Sattar khan st., Tehran, IRAN)

Tehran, Melli Bank, Fakhr Razi Branch: It is located on Enghelab Street - in front of the main door of the University of Tehran .It opened a year ago. According to the gradual change of the banking system in Iran, the first modern banking branch was launched by the National Bank of Iran. The designer pays special attention to performance and beauty so that by creating special features and attracting people's attention, they could encourage them to use new banking systems. Everyone can perform services in certain spaces personally. Its facilities and equipment include:

- New banking system
- Heating and cooling by Duct Split
- Water purifier
- Coffee Shop
- Library
- Web browsing stands
- Free WiFi
- Smart Robot
- Conference room
- Sports space (not yet equipped)

The following points have been carefully considered in the design of this project:

- Use the right colors
- The beauty and fit of the forms
- Transparency of spaces
- Allocation of suitable and sufficient spaces for each function
- Use of appropriate materials
- Proper use of extra spaces
- creation cute views by use flower boxes
- Proper spatial proportions

Table 1. Tehran, Melli Bank, Fakhr Razi Branch

Item	Division	Level of Agreement				
		1	2	3	4	5
	Quality					■
Air	Humidification					■
	Purity				■	
	Quality					■
Water	Treatment				■	
	Drinking Promotion			■		
	Natural access			■		
Light	Color				■	
	Diming		■			
	Collaboration					■
	Quiet Room					■
Mind	On-site child care	-----	-----	-----	-----	-----
	Health and Wellness library					■
	Ergonomics				■	
Comfort	Sound Reduction				■	
	Olfactory Comfort					■
	Fitness Centers	■				
	Stairs				■	
Fitness	Bike Room	-----	-----	-----	-----	-----
	Incentives Programs			■		
	Selection / Availability				■	
Nourishment	Serving Size		■			
	Information		■			
	Venustas / Beauty					■
Architectural Design	Utilitas / Function					■
	Firmitas / Structure					■

Figure 4. Tehran, Melli Bank, Fakhr Razi Branch

5. Results

In this section all the outcomes of the ten case studies are gathered and combined in order to prepare an overlooking perspective toward healthy building contribution in Tehran. The survey includes air, water, light, mind, comfort, fitness, nourishment and "design".

The maximum amount in air indicates 14, in water indicates 12, in light indicates 14, in mind indicates 15, in comfort indicates 13, in fitness indicates 8, in nourishment indicates 8 and in "design" indicates 15. The minimum amount in air indicates 7, in water indicates 5, in light indicates 7, in mind indicates 5, in comfort indicates 8, in fitness indicates 4, in nourishment indicates 7 and in "design" indicates 7.

The comparative analysis emphasized on the role the design elements on the criteria of well building especially "air", "water" and "light". Sustainability is an important part of the design concept in the successful case studies of the research. The results confirmed the role of well-building standard in enhancing the physical and psychological health of the human being. The banks are sample of the indoor environment impacted occupant well-being in an office building.

6. Conclusions

The conclusion highlights that "designing a project based on the function and beauty of architecture" plays an essential role in the quality of the buildings; as well as, the level of satisfaction of the well-building criteria. The designers should be aware of energy consumption and the reduction in carbon emissions from the quantitative analysis for lighting and other energy consuming factors. It in significant to be promoted in the Middle East and North Africa (MENA) region especially.

A designed building tidily resolves many workplace issues, like air condition, vision, comfortable and etc. All of these are subset of seven categories of well building. The conclusion praises the significance of the well Certificate from the International Well Building Institute (IWBI) for measuring human health and well-being of the future buildings in order to be popular in the developing countries such as Iran. The results confirmed the literature that the occupant health has the highest priority, followed by occupant comfort, occupant safety and occupant adaptation.

In bank design, the designer would better focus on well-being and human health within the administrative

Table 2. The Results of the survey

Survey	Air	Water	Light	Mind	Comfort	Fitness	Nourishment	Design
1	11	7	11	6	10	6	7	10
2	8	7	**14**	6	11	**8**	7	**15**
3	**14**	**12**	9	**15**	**13**	**8**	**8**	**15**
4	7	7	8	5	8	5	7	11
5	12	10	10	7	11	7	7	14
6	**8**	5	7	5	8	4	7	7
7	10	9	8	7	10	6	7	13
8	10	9	8	6	9	6	7	11
9	8	7	9	6	8	5	7	10
10	10	9	8	6	10	6	7	11

Table 3. Comparative Analysis Table

Survey	Air	Water	Light
1	10	5	68
2	15	3	76
3	15	1	94
4	11	9	58
5	14	2	78
6	7	10	51
7	13	4	70
8	11	7	66
9	10	8	60
10	11	6	67

building based on the “well Building Standards”. It is building materials that affecting workplace well-being in building construction even in highrise building construction projects and non-high-rise building. Since 2014 when the International Well Building Institute introduced the WELL certification system for assessing human health, well-being and sustainability in buildings until now, our general knowledge enhanced more and more. Right now, it is time to express the necessity of the well Building Standards internationally the developing countries.

Study Limitation

The limitations of this study lie in the expert-based assessment which ignores the audiance. Moreover, another outstanding limitation of the study is the subjective effect which marginized the objective aspects of the well-being.

Conflict of Interest

There is no conflict of interest.

References

[1] Loftness, V., Hakkinen, B., Adan, O., et al., 2007. Elements that contribute to healthy building design. Environmental health perspectives. 115(6), 965-970. DOI: https://doi.org/10.1289/ehp.8988

[2] Spengler, J.D., Chen, Q., 2000. Indoor air quality factors in designing a healthy building. Annual Review of Energy and the Environment. 25(1), 567-600. DOI: https://doi.org/10.1146/annurev.energy.25.1.567

[3] Mohtashami, N., Mahdavinejad, M., Bemanian, M., 2016. Contribution of city prosperity to decisions on healthy building design: A case study of Tehran. Frontiers of Architectural Research. 5(3), 319-331. DOI: https://doi.org/10.1016/j.foar.2016.06.001

[4] D’Amico, A., Pini, A., Zazzini, S., et al., 2020. Modelling VOC emissions from building materials for healthy building design. Sustainability. 13(1), 184. DOI: https://doi.org/10.3390/su13010184

[5] Darwish, B.H., Rasmy, W.M., Ghaly, M., 2022. Applying “well building standards” in interior design of administrative buildings. Journal of Arts & Architecture Research Studies. 3(5), 67-83. DOI: https://doi.org/10.47436/JAARS.2022.124889.1073

[6] Ajiboye, P., Garnys, V., Cash, G., 2022. Applying NABERS IE to a University Building in the UK. In-ASHRAE Topical Conference Proceedings. pp. 1-8. American Society of Heating, Refrigeration and Air Conditioning Engineers, Inc.. https://www.proquest.com/openview/c954ccde848d963d7a65b1ecdf-3d858a/1?pq-origsite=gscholar&cbl=5014767.

[7] Melnick, H., García, E., Leung-Gagné, M., 2022. Building a Well-Qualified Transitional Kindergarten Workforce in California: Needs and Opportunities. Learning Policy Institute. https://learningpolicyinstitute.org/sites/default/files/product-files/California_Transitional_Kindergarten_Workforce_BRIEF.pdf.

[8] Rani, H.A., Radzi, A.R., Alias, A.R., et al., 2022. Factors Affecting Workplace Well-Being: Building Construction Projects. Buildings. 12(7), 910. DOI: https://doi.org/10.3390/buildings12070910

[9] Dunn, H.L., 1959. High-level wellness for man and society. American journal of public health and the nations health. 49(6), 786-792. https://ajph.aphapublications.org/doi/pdf/10.2105/AJPH.49.6.786.

[10] Pressman, S.D., Cohen, S., 2005. Does positive affect influence health?. Psychological bulletin. 131(6), 925. https://psycnet.apa.org/buy/2005-15687-004.

[11] Ostir, G.V., Markides, K.S., Black, S.A., et al., 2000. Emotional well□being predicts subsequent functional independence and survival. Journal of the American Geriatrics Society. 48(5), 473-478. DOI: https://doi.org/10.1111/j.1532-5415.2000.tb04991.x

[12] Ostir, G.V., Markides, K.S., Peek, M.K., et al., 2001. The association between emotional well-being and the incidence of stroke in older adults. Psychosomatic medicine. 63(2), 210-215. https://journals.lww.com/psychosomaticmedicine/Abstract/2001/03000/The_Association_Between_Emotional_Well_Being_and.3.aspx.

[13] Fredrickson, L.B., Levenson, R.W., 1998. Positive emotions speed recovery from the cardiovascular sequelae of negative emotions. Cognition & emotion. 12(2), 191-220. DOI: https://doi.org/10.1080/026999398379718

[14] Tharim, A.H., Ahmad, A.C., Saarani, P.S., et al., 2022. The determinant factors of biophilic design strategies and occupants’psychological performance in office building. Malaysian Journal of Sustainable Environment. 9(3), 87-106. DOI: https://doi.org/10.24191/myse.v9i3.18292

[15] Mansor, R., Sheau-Ting, L., 2022. A measurement model of occupant well-being for Malaysian office building. Building and Environment. 207, 108561. DOI: https://doi.org/10.1016/j.buildenv.2021.108561

[16] McLeod, R.S., Mathew, M., Salman, D., et al., 2022. An investigation of indoor air quality in a recently refurbished educational building. Frontiers in Built Environment. 156. https://static.frontiersin.org/articles/10.3389/fbuil.2021.769761/full.

[17] Mahmoud, N.S., El Samanoudy, G., Jung, C., 2022. Simulating the natural lighting for a physical and

mental Well-being in residential building in Dubai, UAE. Ain Shams Engineering Journal. 29, 101810.
DOI: https://doi.org/10.1016/j.asej.2022.101810

[18] Wang, M., Li, L., Hou, C., et al., 2022. Building and health: Mapping the knowledge development of sick building syndrome. Buildings. 12(3), 287.
DOI: https://doi.org/10.3390/buildings12030287

[19] Schwartz, E.K., Krarti, M., 2022. Review of Adoption Status of Sustainable Energy Technologies in the US Residential Building Sector. Energies. 15(6), 2027.
DOI: https://doi.org/10.3390/en15062027

[20] Houser, K.W., Esposito, T., Royer, M.P., et al., 2022. A method and tool to determine the colorimetric and photobiological properties of light transmitted through glass and other optical materials. Building and Environment. 215, 108957.
DOI: https://doi.org/10.1016/j.buildenv.2022.108957

[21] Chaigneau, T., Coulthard, S., Daw, T.M., et al., 2022. Reconciling well-being and resilience for sustainable development. Nature Sustainability. 5(4), 287-293. https://www.nature.com/articles/s41893-021-00790-8.

[22] Hayawi, Z., 2022. Building a proposed mentoring program of emotional rational programme for lowering theFuture Anxeity of college of education for human sciences and pure sciences. Nasaq. 34(3). https://www.iasj.net/iasj/article/239266.

[23] Hashemin, S., Kazemi, A., Bemanian, M., 2020. Examining the Influence of Healing Garden on Mental Health of the Patients by Emphasizing Stress Reduction. Journal of Environmental Science and Technology. 21(12), 263-276.
DOI: https://doi.org/10.22034/jest.2020.27268.3636

[24] Mohtashami, N., Mahdavinejad, M., Bemanian, M., 2016. Contribution of city prosperity to decisions on healthy building design: A case study of Tehran. Frontiers of Architectural Research. 5(3), 319-331.
DOI: https://doi.org/10.1016/j.foar.2016.06.001

[25] Rasoolzadeh, M., Moshari, M., 2021. Prioritizing for Healthy Urban Planning: Interaction of Modern Chemistry and Green Material-based Computation. Naqshejahan - Basic Studies and New Technologies of Architecture and Planning. 11(1), 94-105. [Persian]
DOI: https://dorl.net/dor/20.1001.1.23224991.1400.11.1.7.0

[26] Shams, G., Moshari, M., 2022. Health and Post-Corona: Air Filtration through Building Skins as Biological Membranes. Naqshejahan - Basic studies and New Technologies of Architecture and Planning. 11(4), 44-59. [Persian]
DOI: https://dorl.net/dor/20.1001.1.23224991.1400.11.4.3.2

[27] Yazhari Kermani, A., Nasrollahi, F., Mahdavinejad, M., 2018. Investigation of the relationship between depth of overhang and amount of daylight indicators in office buildings of Kerman city. Environmental Health Engineering and Management Journal. 5(3), 129-136.
DOI: https://doi.org/10.15171/EHEM.2018.18

[28] Leng, S., 2022. Redesign of ZEB Lab building, NTNU-prioritising passive climate control & comparison with existing (Master's thesis, NTNU). https://ntnuopen.ntnu.no/ntnu-xmlui/handle/11250/3007024.

[29] Raines, E., 2022. The Importance of the WELL Building Standard in Workplace Design. https://keep.lib.asu.edu/items/165640.

[30] Tan, C.Y., Rahman, R.A., Xia, B., et al., 2022. Streamlining WELL Concepts of Office Buildings for Developing Countries: The Case of Malaysia. Construction Research Congress. pp. 606-616. https://www.researchgate.net/profile/Rahimi-A-Rahman/publication/359066619_Streamlining_WELL_Concepts_of_Office_Buildings_for_Developing_Countries_The_Case_of_Malaysia/links/62327c96d37dab4f96eb0936/Streamlining-WELL-Concepts-of-Office-Buildings-for-Developing-Countries-The-Case-of-Malaysia.pdf.

[31] Yamak, F.B., Doğan, E., 2022. Evaluation of WELL Covid-19 Certificate Structure and Criteria. Kent Akademisi. 15(1), 51-63.
DOI: https://doi.org/10.35674/kent.1023057

[32] Wienk, R., 2022. Using Websites as Purposive Sample: An Analysis of How White Supremacist Hate Groups Frame Slavery.
DOI: https://dx.doi.org/10.4135/9781529601589

[33] Ayu, A., Syarifuddin, S., 2022. Keterlibatan Pengguna, Budaya Organisasi Dan Kompetensi Pengguna Terhadap Kualitas Sistem Informasi Akuntansi. AKUA: Jurnal Akuntansi dan Keuangan. 1(3), 261-268.
DOI: https://doi.org/10.54259/akua.v1i3.932

[34] Thomas, F.B., 2022. The Role of Purposive Sampling Technique as a Tool for Informal Choices in a Social Sciences in Research Methods. https://justagriculture.in/files/newsletter/2022/january/47.%20The%20Role%20of%20Purposive%20Sampling%20Technique%20as%20a%20Tool%20for%20Informal%20Choices%20in%20a%20Social%20Sciences%20in%20Research%20Methods.pdf.

[35] Gutierrez, J.M., Yandug, J.S., 2022. Focused Sampling Orientation: Strategy for Quality Assurance in Company XYZ. https://ieomsociety.org/proceedings/2022istanbul/771.pdf.

Journal of Architectural Environment & Structural Engineering Research
https://ojs.bilpublishing.com/index.php/jaeser

ARTICLE

Mechanical and Microstructural Analysis of Waste Ceramic Optimal Concrete Reinforced by Hybrid Fibers Materials: A Comprehensive Study

Hadee Mohammed Najm* Shakeel Ahmad Rehan Ahmad Khan

Department of Civil Engineering, ZH College of Engineering and Technology, Aligarh Muslim University, Aligarh, UP-202002, India

ARTICLE INFO

Article history
Received: 7 July 2022
Revised: 8 August 2022
Accepted: 22 August 2022
Published Online: 1 September 2022

Keywords:
Hybrid fibers
Hooked end steel fiber
Crimped steel fiber
Polyvinyl alcohol fibers
Waste ceramic optimal concrete

ABSTRACT

Combining different types of fibers inside a concrete mixture was revealed to improve the strength properties of cementitious matrices by monitoring crack initiation and propagation. The contribution of hybrid fibers needs to be thoroughly investigated, considering various parameters such as fibers type and content. The present study aims to carry out some mechanical and microstructural characteristics of Waste Ceramic Optimal Concrete (WOC) reinforced by hybrid fibers. Reinforcement materials consist of three different fiber types: hook-ended steel fiber (HK), crimped steel fiber (CR) and polyvinyl alcohol (PVA) fibers and the effect of their addition on the waste ceramic composites' mechanical behaviour. Furthermore, a microstructural analysis was carried out to understand the waste ceramic matrix composition and its bonding to hybrid fibers. Results showed that the addition of hybrid fibers improved the strength characteristics of the ceramic waste composites. For instance, the existence of PVA-CR increased the tensile and flexural strength of the waste ceramic composite by 85.44% and 70.37%, respectively, with respect to the control sample (WOC). As well as hybrid fiber exhibits improved morphological properties as a result of increased pore filling with dense and compact structure, as well as increased C–H crystals and denser structure in pastes as a result of the incorporation of hybrid fibers into the concrete mix. The present experimental research shows the choice of using steel fiber with PVA as a reinforcement material. The idea of adding hybrid fiber is to prepare the economic, environmental, and technological concrete. Moreover, it offers a possibility for improving concrete's durability, which is vital. Finally, it was concluded that steel fiber is more durable, and stiffer and provides adequate first crack strength and ultimate strength. In contrast, the PVA fiber is relatively flexible and improves the post-crack zone's toughness and strain capacity.

*Corresponding Author:
Hadee Mohammed Najm,
Department of Civil Engineering, ZH College of Engineering and Technology, Aligarh Muslim University, Aligarh, UP-202002, India;
Email: gk4071@myamu.ac.in

DOI: https://doi.org/10.30564/jaeser.v5i3.4794

1. Introduction

Concrete can be described as a hard material with low-straining bulk. Reinforcing the concrete using small and randomly distributed fibres could address different issues such as the brittleness and the poor residence to crack of the concrete. In this regard, Kim and Park [1] refer to the significance of enhancing the concrete strength. They indicated that utilising the fibre in concrete will be an effective way to for filling the spacing and that will strengthen the concrete.

Banthia, N., et al. [2] state that applying the fibre in concrete provides enforcement at one and limited range of strain. Thus, several kinds of fiber with changes in constitutive responses, sizes, and functions must be combined to achieve an optimal response. The resulting fibre reinforced concrete mixture is frequently referred to as hybrid FRC, or HyFRC for short.

Regardless of all the mentioned above regarding the fibre efforts in the reinforced concrete, the mixing of the fibre to get a perfect performance of concrete is still quite limited, all the previous studies emphasised on normal or high-performance concrete's mechanical behaviour with hybrid fibers only. While the present study focuses on ceramic waste optimal concrete with hybrid fibers and there is no available data to demonstrate waste ceramic concrete reinforced by hybrid fiber and tested under compression, tension, flexure and combined (flexure and torsion). There is also a great deal of current interest in Synthetic fibers such as PVA & PP, and its performance in HyFRC has never been investigated. Accordingly, this study was undertaken to combine steel (Hooked ended and Crimped) and PVA-fibers in HyFRC and to assess the response under CS, TS, FS & FTS.

Waste ceramic optimal Concrete (WOC) is mainly related to the economic and sustainable concrete with improved mechanical properties (mechanical strength, durability, elasticity modules, etc.). The WOC can be prepared by the addition of waste ceramic as replacement of cement and aggregate (fine and coarse) concerning the size limitation for the maximum size of aggregates and cement (10 mm, 20 mm, and 75 micros) [3].

In terms of waste sutilisations which become a significant problem in recent times, waste ceramics may be used in place of cement and (fine and coarse) aggregate in the concrete mixes. In this way, it can eliminate environmental pollution and create value-added products. For example, in India, recently, an enormous quantity of ceramic waste tiles is produced. Therefore, nowadays, the study is mainly focused on reusing or recycling and recovering waste materials with the help of different applications; it has become the most important topic for research papers. For example, ceramic wastes as a result of tiles production, have been employed to be used as substitutes for coarse aggregate in concrete Keshavarz & Mostofinejad [4]. Also, A. Heidari & Tavakoli [5] has focused on using ceramic waste tiles as a Pozzolanic material in concrete. Torkittikul, & Chaipanich [6] studied the uses of ceramic waste tiles to replace fine aggregate (sand) for manufacturing mortar and concrete. Awoyera et al. [7] has focused on the mechanical properties of ceramic waste floors and wall tiles to replace aggregate in concrete.

Concrete with ceramic waste has economic efficiency, good flexural, and compression strength. It is inherently brittle and has low elasticity, low tensile strength, and low cracking resistance. To overcome the shortcomings of standard concrete, reinforced concrete was developed by incorporating two types of metallic fiber (crimped steel fiber and hook ended steel fiber) and non-metallic fiber (polyvinyl alcohol fiber and polypropylene fiber), was randomly dispersed discontinuously in the concrete. Since randomly dispersed fiber inhibits crack growth and propagation, fiber reinforced concrete has significantly higher

Most of the fiber-reinforced concrete used in experimental work contains only one type of fiber such as Crimped steel fiber with length 50 mm [8], Hook Ended steel fiber with length 60 mm [9] Polyvinyl Alcohol fiber with length 12 mm, Polypropylene fiber (PP) with length 12 mm [10].

The fiber may be combined for optimal response. So, in hybrid concretes, one fibre type is more durable and stiffer that providing the first crack strength and ultimate strength. In contrast, the second type of fiber is relatively flexible and improves toughness and stress capacity in the post-cracking zone [2].

To improve the brittle fracture characteristics and crack control and low tensile strength of concrete, research on fiber reinforced concrete has been steadily attracting attention since the 1960s. The initial researches on the mechanical properties of fiber-reinforced concrete focused on concrete using steel fibers only. It then expanded to studies using various synthetic fibers such as aramid and polyethene from the early 1980s. These fiber-reinforced concretes are generally limited to single fibers, but gradually, to secure high toughness along with crack control of concrete, starting in the late 1990s, hybrid fiber-reinforced concrete mixed with two or more fibers was developed.

Most studies on hybrid fiber reinforced concrete have been concentrated on high-performance concrete, which is being used in industries & lack behind in terms of economy and workability. In contrast, the current study focuses on waste ceramic optimal concrete with hybrid fibers (volume ratio 1% and 2%) [1].

Mixing of different fibers or using hybrid fibers of the same type having different lengths can effectively control the growth of cracks and improve the tensile strength of concrete. The hybridisation of fibers with different material properties effectively increases the strength and ductility of concrete, and the hybridisation of fibers of different lengths effectively controls micro-crack and macro-cracks. It is the most commonly used fiber in the field, although it reduces the flow of concrete and is very effective in improving strength and ductility.

Polyvinyl alcohol (PVA) fiber is a hydrophilic material that does not deteriorate the fluidity of concrete more severely and has low rigidity. It has good dispersibility while mixing concrete and is effective in controlling fine cracks. The hybridisation of steel-PVA fiber effectively secures concrete fluidity and increases strength and ductility.

According to Acikbas & Yaman [11] the combination of two types of matrix or two different types of reinforced materials will result in hybrid concrete, that is one of the classes of composite material.

The improvement of concrete mechanical properties results from concrete reinforcement with a single type of fiber, and has found in a limited range. In contrast, hybrid concrete with two or more types of fiber provides superior properties because cracks occur on various levels and in different sizes. Using several types of fiber with different lengths is the correct way to solve this problem. A good interactive relation between fibers, which is a well-designed composite system, creates the result in improving hybrid performances than mono fiber composite [12].

Tabatabaeian et al. [13] focused on the mechanical properties of hybrid fiber in the mixes of concrete where he used hook end steel fiber and crimped steel fiber both at the same time. Mechanical properties of concrete such as modulus of rupture, compressive strength, flexural strength, and tensile strength were tested. As a result, a slight increase was found in the compressive strength of hybrid concrete. While the modulus of rupture and tensile strength increased dramatically compared to the control specimens, this was because of the active use of steel fiber to control the crack propagation, reducing its growth, and providing a higher contact surface area was attributed.

Kim, & Park [14] examined hybrid fiber reinforced concrete with two types of synthetic fibers, i.e., polypropylene fiber (PP) and polyvinyl alcohol fiber (PVA) were considered in the study. The final results showed that PVA-hybrid fiber concrete had better properties than PP- hybrid fiber concrete. It was attributed to stronger hydrogen bonding by the hydrophilic PVA fiber, which led to superior resistance to crack propagation and microcracking.

It has been observed in the literature that there are existing experimental works to predict the behaviour of ceramic concrete or hybrid fiber concrete [15-24]. However, there is no available experimental work to evaluate the effect of adding Hooked end steel fiber (HK) +polyvinyl alcohol (PVA) or Crimped steel fiber (CR) + polyvinyl alcohol (PVA) with waste ceramic materials on the mechanical properties of concrete, as well as find out the optimal hybridisation of Hooked end steel fiber (HK) +polyvinyl alcohol (PVA) or Crimped steel fiber (CR) + polyvinyl alcohol (PVA), which is important to investigate under different loadings (Compressive, tensile, flexural and torsion); this study can be used to be a reference for future studies and provide extensive data for hybridisation of fibers with ceramic materials studies.

The rest sections of this paper are organised as follows. Research significance is briefly introduced in section 2. In section 3, experimental work is described in detail which include description of materials used, preparation of specimens & mix proportions. In section 4 results and discussion of the experimental results are analysed and discussed as effect of PVA-HK and PVA-CR hybrid fiber on compressive strength, tensile strength, flexural strength & combined flexural and torsion strength of WOC. Finally, conclusions are given in section 5.

Finally, the present research article highlights the following:

- The study focused on the mechanical and microstructural properties of waste ceramic optimal concrete (WOC) with hybrid fibers HK, CR and PVA.
- The study aimed to find out the optimal hybridisation of Hooked end steel fiber (HK) +polyvinyl alcohol (PVA) or Crimped steel fiber (CR) + polyvinyl alcohol (PVA).
- In hybridisation, one fibre type is more durable and stiffer than providing the first crack strength and ultimate strength and the second type of fiber is relatively flexible and improves toughness and stress capacity in the post-cracking zone.
- The results of the study have expected to add the knowledge guideline on the use of ceramic waste material to alleviate the negative ceramic impact on the environment and contribute to sustainable concrete production.

2. Research Significance

Fracture in concrete is a gradual, multi-scale process, occurring at both the micro and the macro levels. For fiber reinforced concrete, therefore, is very limiting when only one type and dimension of fiber is used as reinforcement. Such reinforcement clearly restricts crack growth at its own scale and has little or no influence on fracture processed at other scales. For maximum reinforcing efficiency, fibers of various types must be combined in a rational manner. In this paper, WOC-hybrid fiber reinforced concrete mixes carrying various combinations of steel and PVA fibers were studied under compression, tension, flexural and combined (flexural and torsion) loading, and performance was investigated.

3. Materials and Methods

3.1 Materials

The materials used in this study included Ordinary Portland Cement (OPC) 43-grade, Natural Coarse Aggregate (NCA)/stones, coarse river sand, ceramic floor tiles with three types of fiber Hook End Steel Fiber (HK), Crimped Steel Fiber (CR), and Polyvinyl Alcohol Fiber have been used as described below.

3.1.1 Cement

In this study, two types of cement were used the first one was 43 grade of Ordinary Portland Cement (OPC) conforming to IS: 8112-1989 and the second one waste ceramic cement (C_{WC}). The main constituents of OPC (43 grade) and C_{WC} are lime-silica (calcium silicate) compounds. The laboratory tests were conducted to determine the physical properties of OPC and CWC according to IS codes. Tables 1 & 2 summarises the chemical and physical properties of OPC (43 grade) and C_{WC}.

3.1.2 Aggregate

In this study, two types of aggregate have been used, the first one was natural aggregate and the second one was ceramic aggregate. Ceramic has been used in both as coarse aggregate (A_{WC}) and fine aggregate (S_{WC}). Ceramic aggregate is very compact with a low porosity but high strength. As the latest product of ceramic technology, it's manufactured from clay, feldspar, or granite and silica under high pressure and heat for use as flooring and façade material in buildings because of its beauty, strength properties and heat resistance.

Baking at high temperatures makes ceramics vitreous with low porosity and extremely low water absorption, often termed as artificial stones. Due to their very high strength, they cannot be easily recycled back into the manufacturing line and are, therefore, generally dumped and released as waste into the environment. It is, therefore, desirable to find ways to reuse them in beneficial ways.

Aligarh's Ceramic Stores provided the waste ceramic floor tiles that were used in this project. Ceramic tiles were cleaned and dusted off before being hammered into various sizes: 20 mm and 10 mm (waste ceramic aggregate- A_{WC}); 4.75 mm (waste ceramic sand- S_{WC}) (Figures 2 & 3).

Both aggregates were graded according to IS code as shown in Figures 1 & 2. The natural and ceramic aggregates thus obtained were characterised in terms of normal consistency, specific gravity, finesse modules, maximum size, density (kg/m³), water absorption, crushing value and impact value as reported in Table 1.

3.1.3 Fibers

Three types of reinforcement materials, including Hook End Steel Fiber (HK), Crimped Steel Fiber (CR), and Polyvinyl Alcohol Fiber (PVA) have been used as shown in Figure 3 & Table 3. PVA fiber is a hydrophilic material having a hydroxyl group. It has excellent adhesion to cement matrix, excellent dispersibility, and is a micro synthetic short fiber with a diameter of 0.04 mm. Steel fibers are cut in pieces from manufactured bundles so that they are easily dispersed when mixed with concrete and have hooks at both ends to improve adhesion and fixing performance with cement matrix. Table 3 shows the properties of fibers used.

(a) (b) (c) (d)

Figure 1. (a) Commercial cement; (b) river sand; (c) natural coarse aggregates (NCA)—10 mm; (d) natural coarse aggregates (NCA)—20 mm.

(a) (b) (c) (d)

Figure 2. (a) waste ceramic cement (C_{WC})-75µm (b) waste ceramic sand (S_{WC})-4.75 mm (c) waste ceramic aggregate (A_{WC})-10 mm (d) waste ceramic aggregate (A_{WC})20 mm

(a) (b) (c)

Figure 3. metallic and non-metallic fiber: (a) Crimped Steel fiber (CR; 60 mm) (b) Hook Ended steel fiber (HK; 60 mm) (c) Polyvinyl Alcohol fiber (PVA; 12 mm)

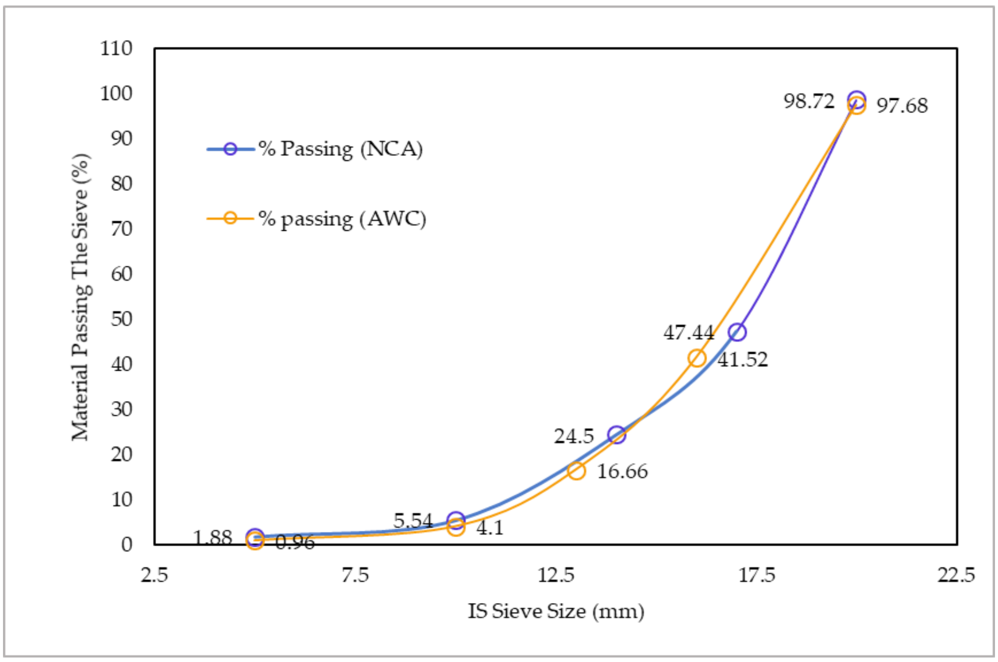

Figure 4. Particle Size Distribution of Natural Coarse Aggregate & Ceramic Coarse Aggregate

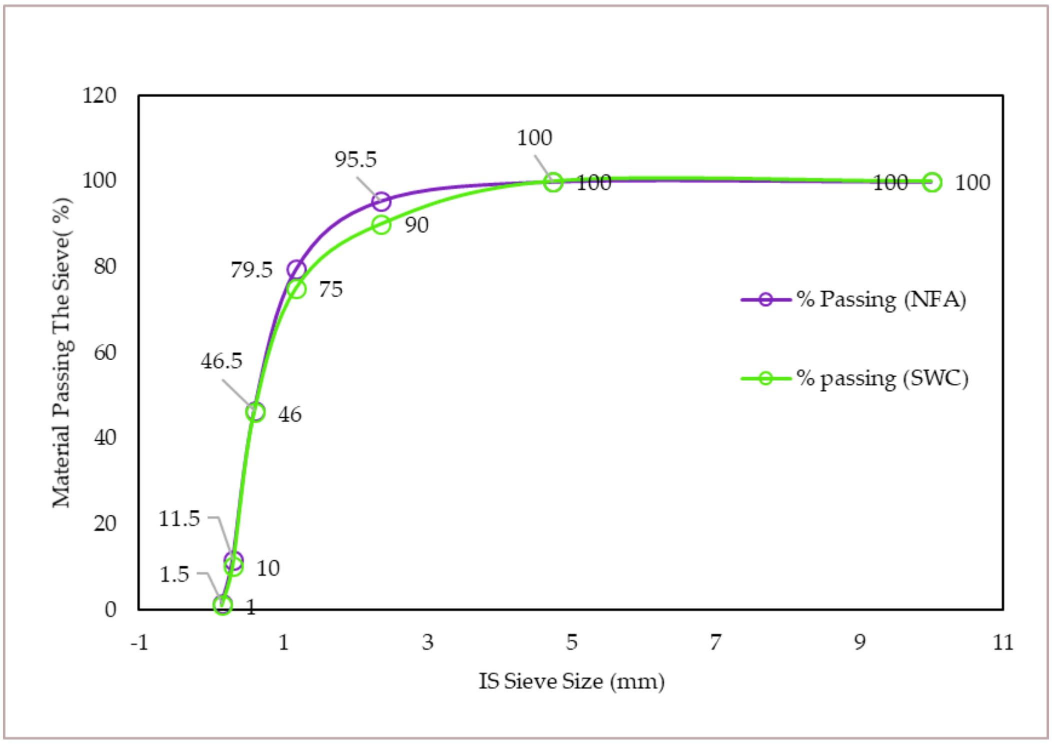

Figure 5. Particle Size Distribution of Natural Fine Aggregate & Ceramic Fine Aggregate

Table 1. Properties of Used Material

Physical Properties	**Cement – OPC**	**NCA**	**Sand**	**C_{WC}**	**A_{WC}**	**S_{WC}**
Normal consistency (%)	32	-	-	8	-	-
Specific Gravity	3.15	2.84	2.64	2	2.31	2.26
Initial setting time	42 minute	-	-	54 minutes	-	-
Final setting time	600 minute	-	-	680 minutes	-	-
7 days compressive strength	21.1 MPa	-	-	37	-	-
Finesse modules	-	6.99	2.65	-	6.98	2.2
Maximum Size	75 µm	0.02 m	4.75 mm	75 µm	0.02 m	4.75 mm
Density (kg/m³)	1440	1550	1650	-	-	-
Water Absorption (%)	-	0.23	2.24	-	0.55	2.52
Crushing value (%)	-	34	-	-	20.86	-
Impact Value (%)	-	24	-	-	27	-
NCA: Natural Coarse Aggregate	A_{WC}: Waste Ceramic Aggregate		S_{WC}: Waste Ceramic Sand		C_{WC}: Waste Ceramic Cement	

Table 2. Chemical Analyses of Waste Ceramic Powder and OPC

Materials	Waste Ceramic Powder (C_{WC})	Cement (OPC 43)
SiO_2	68.85	22.18
Al_2O_3	17	7.35
Fe_2O_3	0.8	3.83
CaO	1.7	63.71
Na_2O	_	0.28
K_2O	1.63	0.11
MgO	2.5	0.95
TiO_2	0.737	0.13
MnO	0.078	0.04
LOI	1.78	1.6

Table 3. Properties of Used Fibers

Fiber Type	CR	PVA
Surface	Plane	-
Cross-section	Circular	-
Anchorage	Continuous	Straight
Length (mm)	50 mm	12 mm
Diameter (mm)	1	0.04
Aspect ratio	50	300
Density (g/cm^3)	7.85	1.3
Tensile strength (MPa)	1250	1560
Elastic modulus (GPa)	200	41

3.2 Mix Design

Overall, 6 phases were carried out in this study as described below:

1) The first phase of mix design includes the control mix with ceramic waste material as a replacement of cement and aggregate (Fine & Coarse) without any addition of single or hybrid fibers named as Waste Ceramic Optimal Concrete (WOC).

2) The second Phase of mix design included the single addition of hook end steel fiber (50 mm length) with a volume ratio 1% named as HK-1-WOC.

3) The third Phase of mix design included the single addition of crimped steel fiber (50 mm length) with a volume ratio 1% named as CR-1-WOC.

4) the Fourth phase of the mix design included the single addition of polyvinyl alcohol fiber (12 mm length) with a volume ratio 1% named as PV-1-WOC.

5) The Fifth phase of the mix design included the hybrid addition of Hook ended steel fiber (1%, 50 mm length) and polyvinyl alcohol fiber (1%, 12 mm length) named as HK-1-WOC.

6) The Sixth phase of mix design included the hybrid addition of Crimped steel fiber (1%, 50 mm length) and polyvinyl alcohol fiber (1%, 12 mm length) named as CR-1-WOC.

*In every phase, 12 specimens have been cast, including 3 cubes, 3 cylinders and 6 beams. 3 cubes were tested under compression, 3 cylinders were tested under tension 3 beams were tested for flexural, and the remaining 3 beams were tested for the combined (flexural and torsional) strength test. Details are shown in Table 4.

Table 4. Description of Phase Testing of Total 72 Test Specimens

phase	Samples	Percentage of Fiber	Purpose of Casting							
			Compressive Strength (Cube)		**Tensile Strength (Cylinder)**		**Flexural Strength (Beam)**		**Combined (Flexure + Torsional) Strength (beam)**	
			N.	**Size (mm)**	**N.**	**Size (mm)**	**N.**	**Size (mm)**	**N.**	**Size (mm)**
Phase 1	WOC	0% of fiber	3	150*150*150	3	150 * 300	3	100*100*500	3	100*100*500
Phase 2	HK-1-WOC	1% of HK steel fiber	3	150*150*150	3	150 * 300	3	100*100*500	3	100*100*500
Phase 3	CR-1-WOC	1% of CR steel fiber	3	150*150*150	3	150 * 300	3	100*100*500	3	100*100*500
Phase 4	PVA-1-WOC	1% of PVA fiber	3	150*150*150	3	150 * 300	3	100*100*500	3	100*100*500
Phase 5	PVA-HK-WOC-2%	1% of PVA fiber and 1% of HK steel fiber	3	150*150*150	3	150 * 300	3	100*100*500	3	100*100*500
Phase 6	PVA-CR-WOC-2%	1% of PVA fiber and 1% of CR steel fiber	3	150*150*150	3	150 * 300	3	100*100*500	3	100*100*500

3.3 Preparation of Specimens

A total of 72 specimens were cast to investigate the mechanical properties of WOC with single and hybrid fiber and find its optimal use. For this purpose, 18 cubes (150 * 150 * 150 mm), 18 cylinders (150 * 300 mm), and 36 beams (100 * 100 * 500 mm) were cast with varying types of fiber (HK, CR and PVA). The specimens were removed from the moulds after 24 hours and placed in a curing tank for 28 days at a temperature of 27 °C. Finally, the specimens were dried for 24 hours before testing. The mix proportions for concrete for different addition of fiber are shown in Table 5.

3.4 Test Procedures

The properties of fresh and hardened WOC and WOC-Hybrid mixes were determined using test procedures adapted from those used for traditional Portland cement-based concrete. Test methods were selected to allow simple characterisation of the mechanical properties of hardened mixes under short-term loading conditions. Table 4 illustrates the details of different phases of mixes and tests. First, the compressive strength test was done to investigate the compressive mechanical property. The second test was the tensile strength test which was conducted to investigate the tensile mechanical property. Then flexural strength test to investigate the flexural mechanical property. Finally, a combined test (flexural and torsion strength) investigated the ultimate bending stress under torsion. The characterisation of all mixtures was carried out through the tests detailed in Table 5.

3.5 Concrete Mix Microstructure

The microstructure and chemical analysis of modified concrete specimens were carried out using scanning electron microscopy (SEM) and energy-dispersive spectroscopy (EDS) techniques. In this study, the scanning electron microscope JSM6510LV (JEOL, Ja-pan) was used, with an accelerating voltage of 30.0 kV. In order to conduct EDS analysis, the surface of samples was ground and polished to an ultra-smooth finish and then coat-ed with carbon or gold. The specimens in this study were coated in gold.

Table 5. Mix Proportion

Mix Ingredients (kg/m^3)						
Material	**WOC**	**HK-1-WOC**	**CR-1-WOC**	**PVA-1-WOC**	**PVA-HK-WOC-2%**	**PVA-CR-WOC-2%**
Water	190	190	190	190	190	190
OPC (43 grade)	342	342	342	342	342	342
C_{WC}	38	38	38	38	38	38
NCA	894	894	894	894	894	894
A_{WC}	224	224	224	224	224	224
Sand	548	548	548	548	548	548
S_{WC}	61	61	61	61	61	61
Weight Proportion Fiber (by Volume of Concrete)						
PVA %	-	-	-	13	13	13
HK %	-	78	-	-	78	-
CR %	-	-	78	-	-	78

Table 5. Testing procedures on ceramic concrete

Tests	Equipment	Sample	Condition	Formula
Slump	Abram cone	Fresh concrete	Immediately after mixing	-
Compressive Strength (IS: 516-1959)	(2000 KN) Compressive Testing Machine at Axial	hardened concrete	After 28 Days of Curing	
Tensile Strength (IS: 516-1959)	(2000 KN) Compressive Testing Machine at Horizontal	hardened concrete	After 28 Days of Curing	
Flexural Strength (IS: 516-1959)	Two-point load test	hardened concrete	After 28 Days of Curing	
Combined Flexural and Torsion Strength (IS: 516-1959)	Two-point load test + Torsion Girder	hardened concrete	After 28 Days of Curing	

4. Results and Discussion

Table 6 summarises the results of the mechanical properties of the mixed hybrid fiber ceramic concrete. The Compressive Strength (CS), Tensile Strength (TS), Flexural Strength (FS) and combined (flexural and torsional) strength (FTS) of concrete has been expressed as a percentage of the reference concrete. In addition, in order to evaluate the properties of hybrid fiber ceramic concrete, these experimental results have been compared with previous studies and with single PVA fiber or single HK and CR steel fiber mixed concrete.

4.1 Effect of PVA-HK and PVA-CR Hybrid Fiber on Compressive Strength of WOC

The compressive strength results of single and hybrid fiber concrete for all specimens at the ages of 28 days are shown in Chart 1 and Table. 6. The previous study shows that the compressive strength of fiber reinforced concrete is significantly influenced by fiber mix, fiber strength, fiber linearity, fiber adhesion, fiber distribution and fiber length. Increasing the fiber volume ratio contributes to increased compressive strength by increasing the resistance to the long transverse strain. On the other hand, microcracks that occur along the load direction during the maximum compressive stress in concrete are over-controlled by short fibers rather than long fibers, so the shorter the fiber length, the better the compressive strength increases.

An increment of 16.07% and 5.52% in CS was observed for HK-1-WOC and CR-1-WOC, respectively, w.r.t WOC. A significant effect has occurred by adding 1% steel fiber (HK or CR) on compressive strength exhibited in WOC concrete. The compressive strength increment is due to steel Fiber's presence, which enhancing mechanical bond strength. The matrix of the steel fiber will supply the delaying microcrack formation and detain the propagation. The increase in the steel fiber volume ratio changed WOC's strength response and allowed the specimens (WOC + fiber) to exhibit greater peak strength than the plain specimens (WOC). Unreinforced concrete (WOC) has shown more brittleness behaviour and the addition of steel fibers to it has shown more ductile fractures.

On the other hand, the compressive strength of hybrid fiber reinforced concrete PVA-CR-WOC and PVA-HK-WOC increased by 16.87%, 21.73% respectively compared to unreinforced concrete (WOC) as shown in Chart 5. The compressive strength of concrete reinforced with PVA fiber and steel fiber was larger than that of concrete reinforced with single steel fiber, it was attributed to stronger hydrogen bonding by the hydrophilic PVA fiber, which led to superior resistance to crack propagation and microcracking.

K. H. Yang [1] has reported more or less similar behaviour for the addition hybrid fiber. The mentioned study has observed that the CS in specimens containing Hybrid fiber (PVA-HK) without ceramic material was enhanced by 17.52% [1]. In contrast, in the present study, specimens containing hybrid fibers (PVA-HK) with ceramic material (PVA-HK-WOC) have been enhanced by 21.73%. This achievement may be due to the effective quantitation of the fibers into the ceramic waste tiles. Figure 4 shows compressive strength test specimens at failure.

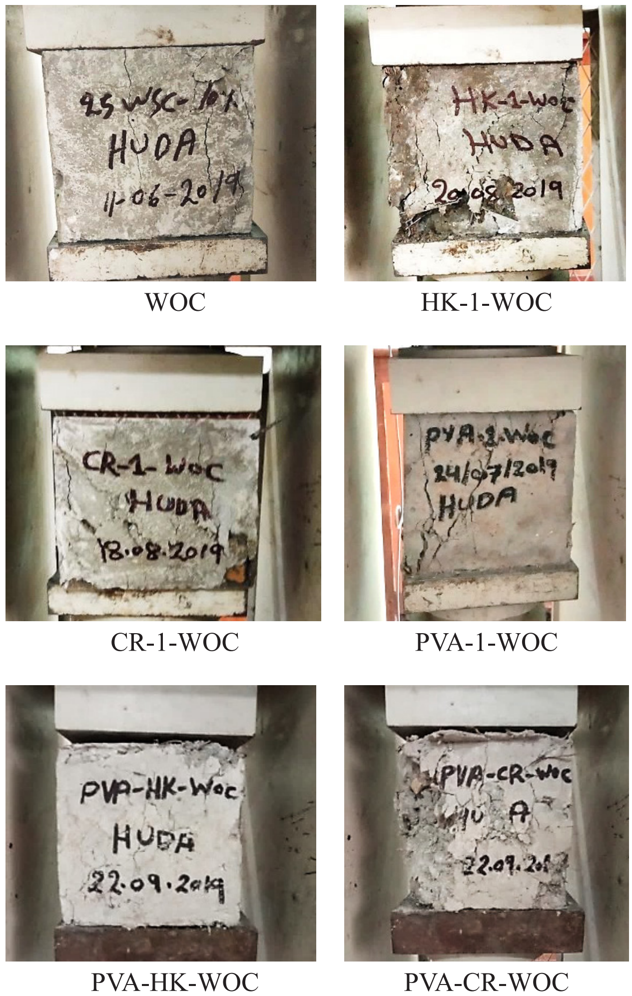

Figure 4. Compression test specimens: WOC, HK-1-WOC, CR-1-WOC, PVA-1-WOC, PVA-HK-WOC and PVA-CR-WOC CR-1-WOC at failure

4.2 Effect of PVA-HK and PVA-CR Hybrid Fiber on Tensile Strength of WOC

One of the easiest and most popular methods for indirect measurement of concrete's tensile strength is the split tensile strength test. The Tensile Strength results of single and hybrid fiber concrete for all specimens at the ages of

28 days are shown in Chart 2 and Table 6.

It can be seen from the results, the improvement in tensile strength by incorporating metallic fiber (HK or CR) and non-metallic fiber (PVA) exhibits a similar trend to that observed for compressive strength. The specimens reinforced with HK, CR, and PVA fiber show excellent enhancement in tensile strength ranging from 34.7% for HK-1-WOC, 50 % for CR-1-WOC, and 30.59% for PVA-1-WOC, respectively.

The results show that metallic fiber (HK or CR) hybridisation with non -metallic fiber (PVA) could improve the tensile strength of WOC concrete specimens. The tensile strength of PVA-HK-WOC and PVA-CR-WOC concrete was enhanced by 55.97% and 85.44%, respectively, compared to the reference model (WOC) as shown in Chart 5.

As compared to compressive strength, the tensile strength is more sensitive to the addition of hybrid fiber and highly effective at the same fibers volume ratio (1% PVA + 1% CR). It must be noted that the hybridisation of concrete by fibers must have two types of fibers, the first type of the used fibers (HK or CR) should be more durable and stiffer which provides the first crack strength and ultimate strength. Whereas the second type of used fibers (PVA) is relatively flexible, and improves toughness and stress capacity in the post-cracking zone.

Yangs [1] has studied the effect of addition hybrid fibers (PVA-HK) on TS of concrete. On the basis of comparison between the mentioned study and the present study, it was observed that the TS in specimens containing hybrid fibers (PVA-HK) without ceramic material was enhanced by 63.36% [1] whereas the specimens containing hybrid fibers (PVA-HK) with ceramic material (PVA-HK-WOC) was enhanced by 55.97%. Figure 5 shows tensile strength test specimens at failure.

4.3 Effect of PVA-HK and PVA-CR Hybrid Fiber on Flexural Strength of WOC

Flexural strength is a needful parameter in assessing single and hybrid fiber's influence on the response of the concrete composites. The flexural strength reflects the ability of energy consumption of concrete after cracking. The flexural strength of single and hybrid fiber concrete is shown in Chart 3 and Table 6.

The addition of single fibers (HK, CR and PVA) improves the flexural strengths of WOC concrete by 33.34% for HK-1-WOC, 40.74% for CR-1-WOC and 9.62% for PVA-1-WOC as shown in Chart 5.

In this study, the flexural strength increased in the hybridisation models. Where the flexural strength was more significant for the addition of hybrid fiber (PVA-CR). The specimens of PVA-HK-WOC and PVA-CR-WOC showed an increment of 48.14% and 70.37%, respectively in the FS w.r.t reference model (WOC) as shown in Chart 5.

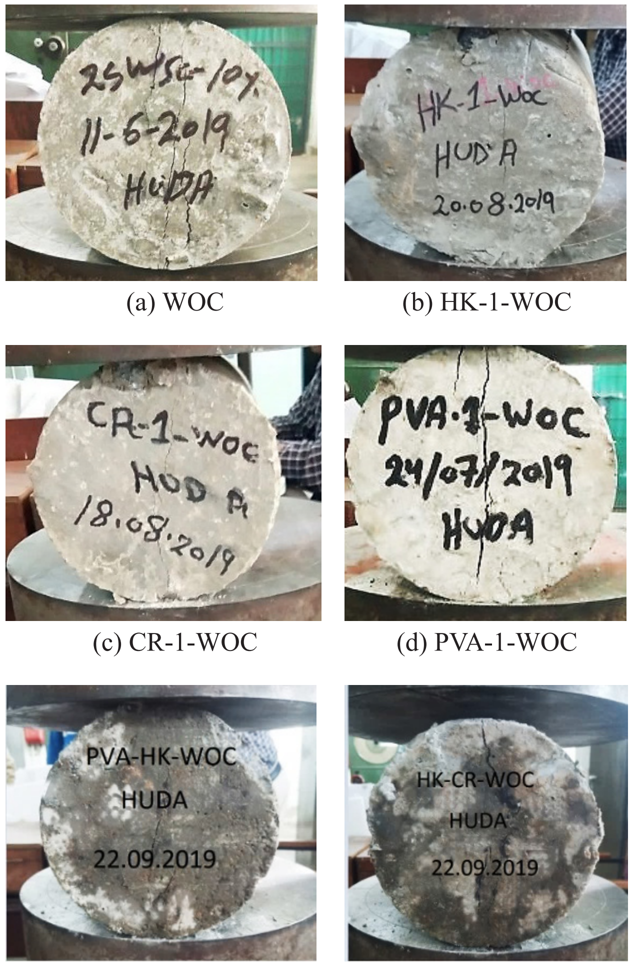

(a) WOC (b) HK-1-WOC

(c) CR-1-WOC (d) PVA-1-WOC

e) PVA-HK-WOC (f) PVA-CR-WOC

Figure 5. Tension test specimens: WOC, HK-1-WOC, CR-1-WOC, PVA-1-WOC, PVA-HK-WOC and PVA-CR-WOC CR-1-WOC at failure

One of the reasons for the higher performance of WOC-Hybrid fiber reinforced concrete is the PVA fibers effectively control the crack propagation at the bending crack tip and the steel fibers resist the widening of the crack width, thereby greatly enhancing concrete's flexural strength.

Yang [1] has reported more or less similar behaviour for the addition hybrid fiber. On the basis of comparison between mentioned study and the present study, it was observed that the FS in specimens containing hybrid fiber (PVA-HK) without ceramic material was enhanced by 61.14% [1] whereas, in specimens containing hybrid fibers (PVA-HK) with ceramic material (PVA-HK-WOC) was enhanced by 48.14%. Figure 6 shows flexural strength test specimens at failure.

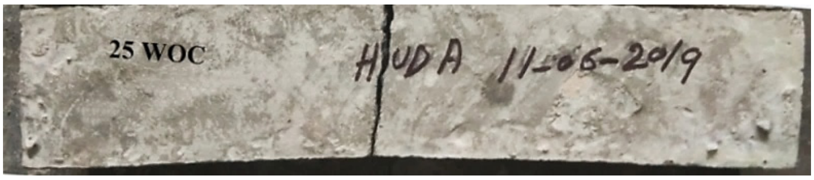

(a) WOC

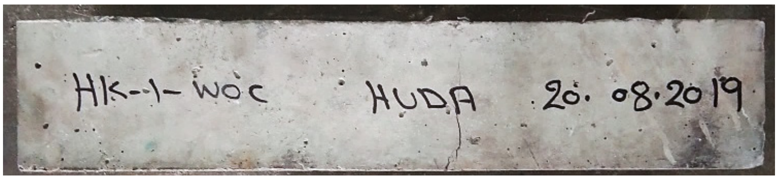

(b) HK-1-WOC

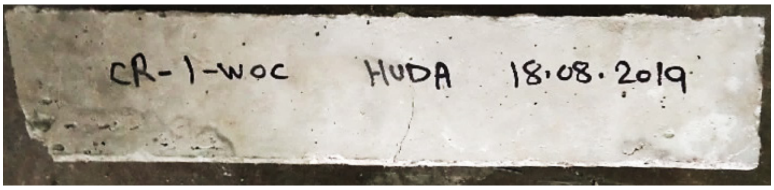

(c) CR-1-WOC

(d) PVA-1-WOC

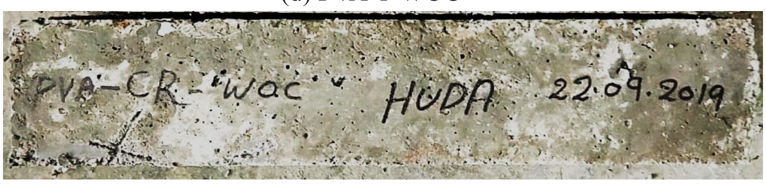

(e) PVA-CR-WOC

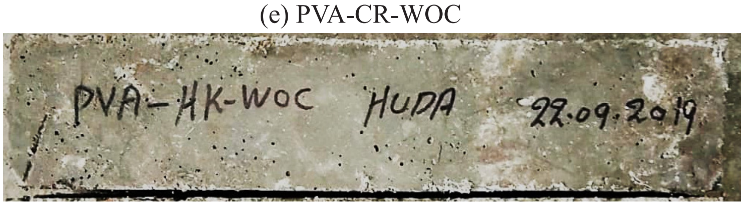

(f) PVA-HK-WOC

Figure 6. Flexural test specimens: WOC, HK-1-WOC, CR-1-WOC, PVA-1-WOC, PVA-HK-WOC and PVA-CR-WOC CR-1-WOC at failure

4.4 Effect of PVA-HK and PVA-CR Hybrid Fiber on the Combined (Flexure and Torsion) Strength of WOC

The results of ultimate bending stress under torsion 243 N.mm, 254 N.mm and 265 N.mm for all specimens of single and hybrid fiber concrete are presented in Chart 4, Chart 5 and Table 6. As compared with the reference specimen (WOC), all the specimens with metallic (HK or CR), non-metallic (PVA), and hybrids fiber (PVA-HK, PVA-CR) have an excellent ultimate bending stress than samples without fiber where:

1) Values of UBS under torsion 243 N.mm for all specimens with single fiber (HK-1-WOC, CR-1-WOC, PVA-1-WOC) were higher than reference concrete (WOC), as 40.74%, 48.15%, and 3.7% respectively. Also, samples of hybrid fiber (PVA-HK-WOC and PVA-CR-WOC) under the same value of torsion have a higher value than reference concrete (WOC) as 55.55% and 77.78%, respectively.

2) Values of UBS under torsion 254 N.mm for all spec-

imens with single fiber (HK-1-WOC, CR-1-WOC, PVA-1-WOC) were higher than reference concrete (WOC), as 41.67%, 50.00%, and 8.33% respectively. Also, samples of hybrid fiber (PVA-HK-WOC and PVA-CR-WOC) under the same value of torsion have a higher value than reference concrete (WOC) as 50.00% and 91.66% respectively.

3) Values of UBS under torsion 265 N.mm for all specimens with single fiber (HK-1-WOC, CR-1-WOC, PVA-1-WOC) were higher than reference concrete (WOC), as 18.18%, 22.73%, and 9.09% respectively. Also, specimens of hybrid fiber (PVA-HK-WOC and PVA-CR-WOC) under the same value of torsion have a higher value than reference concrete (WOC) as 45.45% and 81.81% respectively.

4) specimens reinforced with hybrid (PVA-CR) fiber give the maximum UBS that was estimated as 91.66% higher under torsion 254 N.mm higher in comparison with reference specimen (WOC). It was also shown that specimens reinforced with the hybrid (PVA-HK) fiber demonstrated their effectiveness in providing semi- ductility to a concrete structure. It could be concluded that the UBS with hybrid fiber reinforcements has enhanced significantly, same as in the flexural and tensile strength.

5) Figure 7 shows combined (flexural and torsion) strength test specimens at failure.

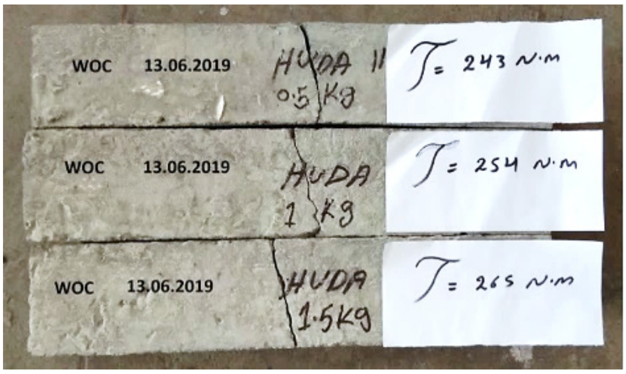

WOC

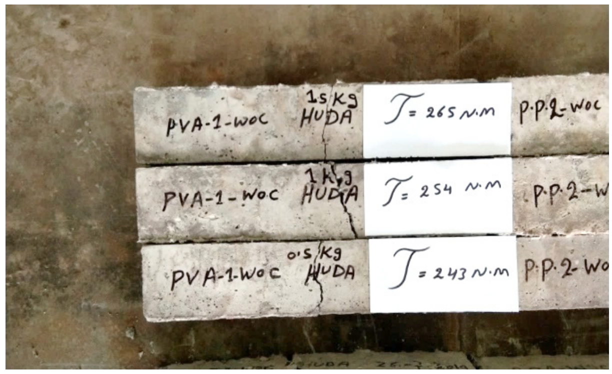
PVA-1-WOC


HK-1-WOC

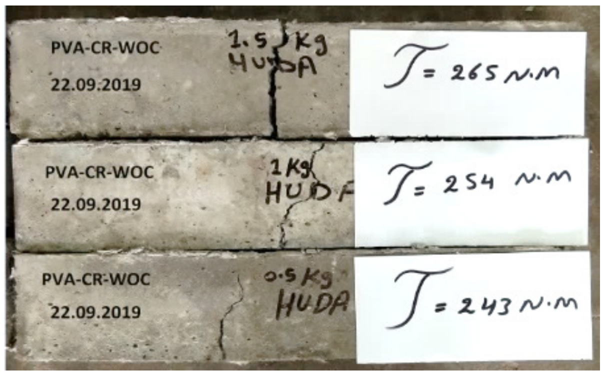

PVA-CR-WOC

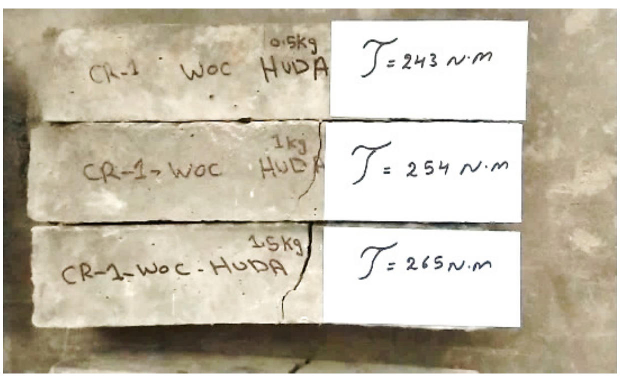
CR-1-WOC

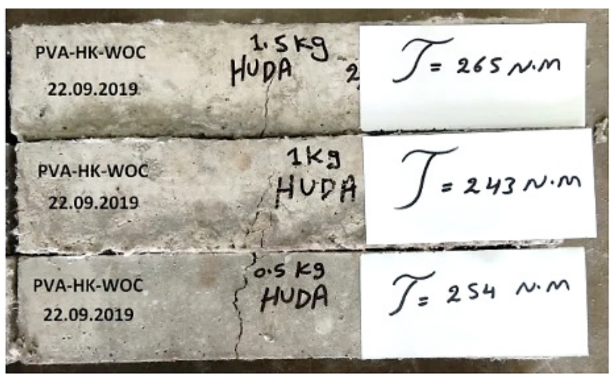

PVA-HK-WOC

Figure 7. Combined (flexural and torsion) strength test specimens: WOC, HK-1-WOC, CR-1-WOC, PVA-1-WOC, PVA-HK-WOC and PVA-CR-WOC CR-1-WOC at failure

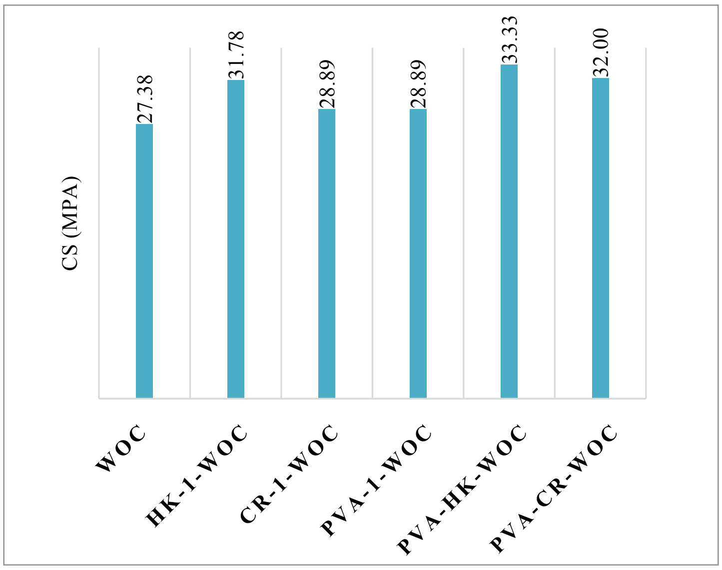

Chart 1. Average compressive strength (CS) for varying mixes with respect to the reference concrete model

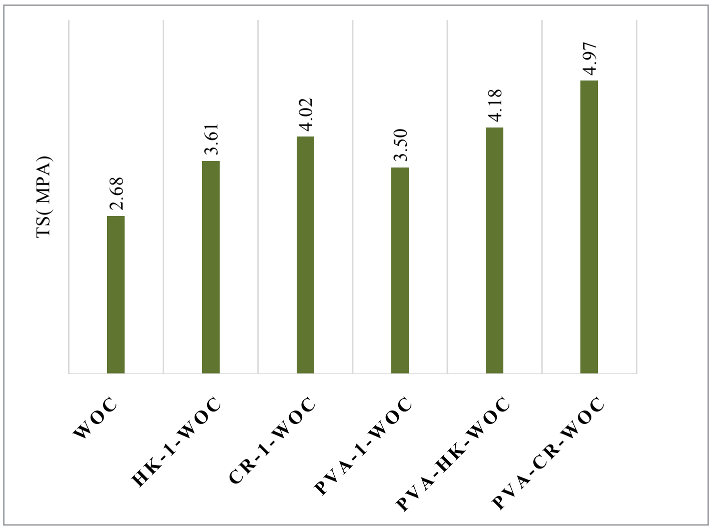

Chart 2. Average split tensile strength (TS) for varying mixes with respect to the reference concrete model

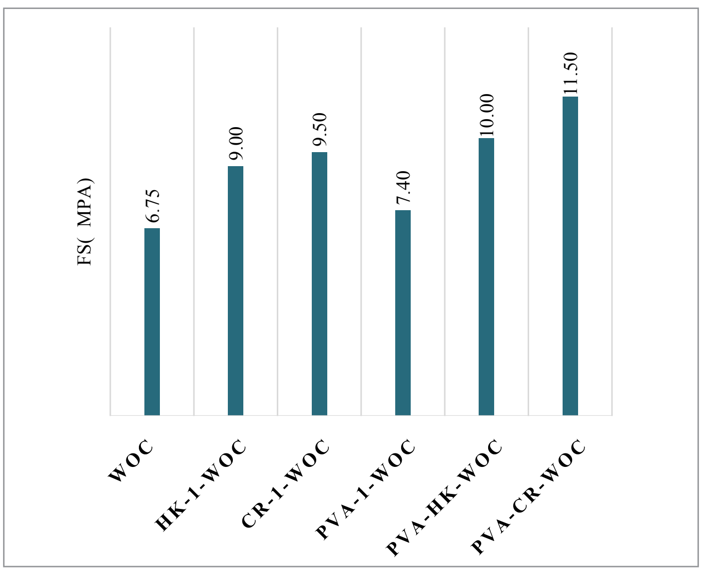

Chart 3. Average Flexural Strength (FS) for varying mixes with respect to the reference concrete model

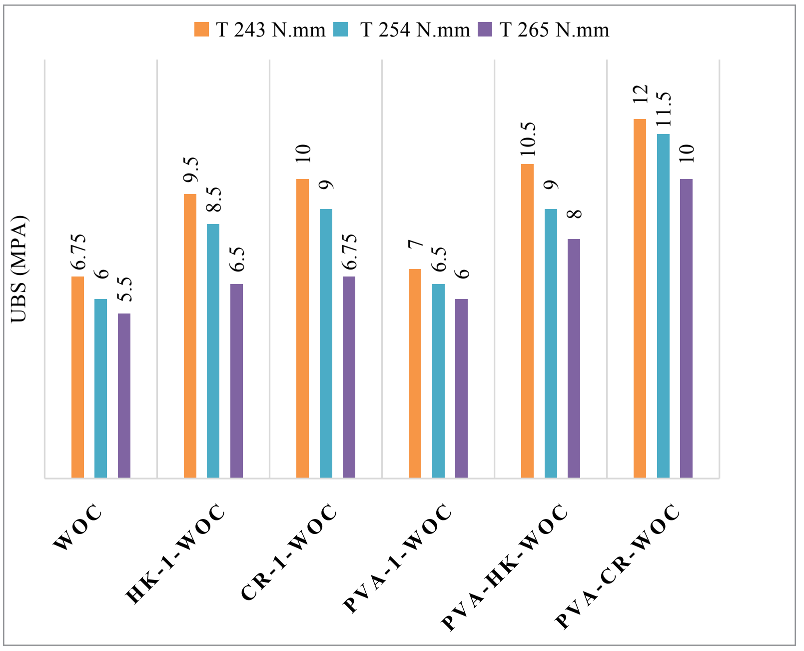

Chart 4. Average ultimate bending strength (UBS) for varying mixes in WOC with respect to the reference concrete model

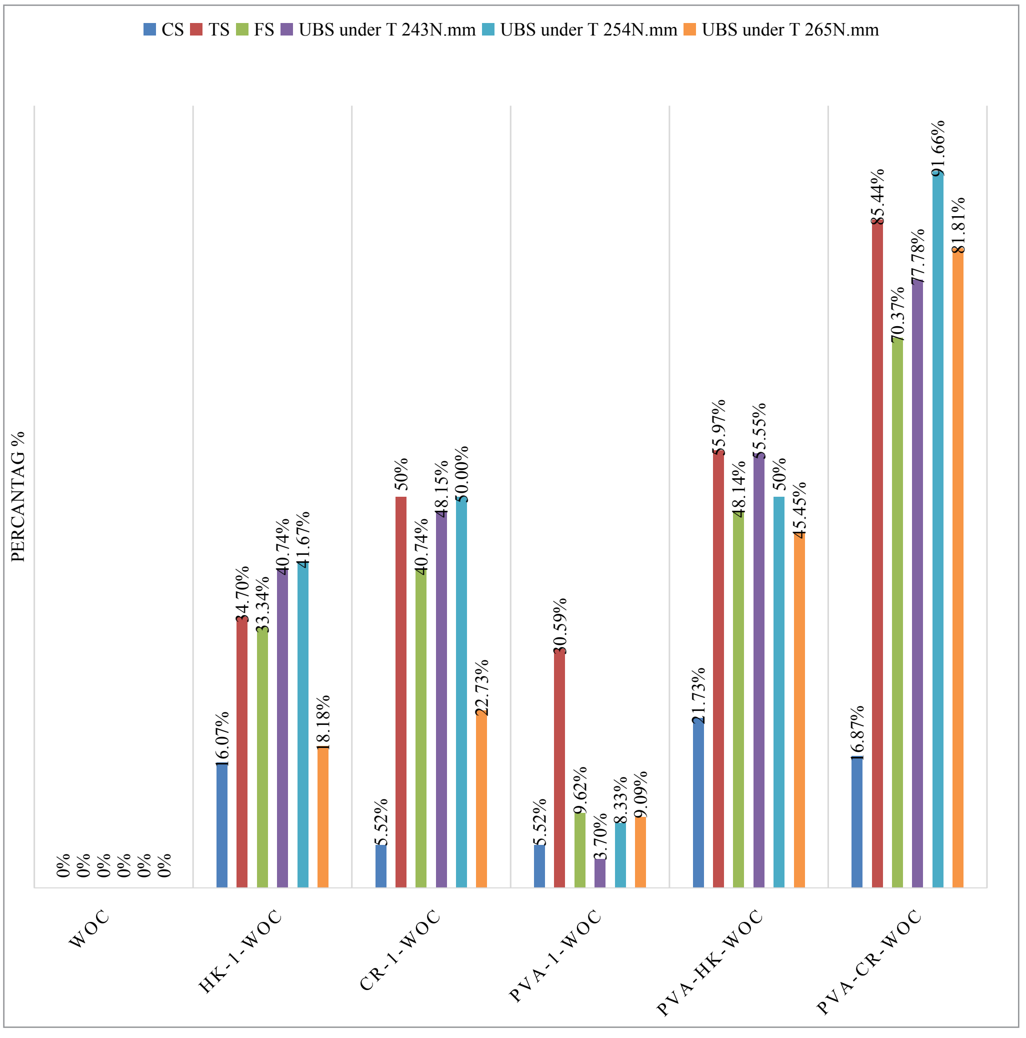

Chart 5. Overall Percentage of increment/ decrement of total tested results

Table 6. Average Compressive, Tensile, Flexural, Combined (Flexural and Torsional) Strength for Various Mixes

S No.	Sample Name	CS (%variation w.r.t to reference)	TS (%variation w.r.t to reference)	FS (%variation w.r.t to reference)	UBS MPa Under Torsion 243 N.mm (%variation w.r.t to reference)	UBS MPa under Torsion 254 N.mm (%variation w.r.t to reference)	UBS MPa Under Torsion 265 N.mm (%variation w.r.t to reference)
		MPa					
1	WOC (Reference)	27.38	2.68	6.75	6.75	6	5.5
2	HK-1%-WOC	31.78 (+16.07%)	3.61 (+34.7%)	9 (+33.34%)	9.5 (+40.74%)	8.5 (+41.67%)	6.5 (+18.18%)
3	CR-1%-WOC	28.89 (+5.52%)	4.02 (+50%)	9.5 (+40.74%)	10 (+48.15%)	9 (+50.00%)	6.75 (+22.73%)
5	PVA-1%-WOC	28.89 (+5.52%)	3.5 (+30.59%)	7.4 (+9.62%)	7 (+3.7%)	6.5 (+8.33%)	6 (+9.09%)
7	PVA-HK-WOC-2%	33.33 (+ 21.73%)	4.18 (+ 55.97%)	10.00 (+ 48.14%)	10.5 (+55.55%)	9 (+50%)	8 (+45.45%)
8	PVA-CR-WOC-2%	32 (+16.87%)	4.97 (+85.44%)	11.50 (+70.37%)	12.00 (+77.78%)	11.5 (+91.66)	10 (+81.81)

+: Increment - : Reduction

4.5 Microstructure Analysis

The analyses of SEM and EDS intended to investigate the morphological properties of plain concrete(pc), waste ceramic optimal concrete (WOC) and waste ceramic reinforced by hybrid fiber (WOC-Hybrid), as shown in Figures 8, 9 and 10. The PC sample is selected as a reference model; the WOC sample is selected based on the optimal performance of each group of ceramic replacements. The WOC-Hybrid sample is selected based on the optimal performance of each group of fiber additions. All the selected samples have taken from failed samples in a compressive strength test.

The SEM micrographs of PC have shown clear visibility of hexagonal plate-shaped crystals of CH and C-S-H gels. The SEM micrographs have also shown a presence of hydrous calcium-aluminate hydrate characterised by a needle-like structure. Several voids, pores, mixed distribution of C-S-H and C-H gel and needle-like ettringite crystal with visible micro-cracks inside the structure have been detected, as shown in Figure 6.

The result of the PC has shown a ceramic particle reacted with prism-shaped columns, which mainly consisted of Al and Si, which means that both components are the main chemical reaction that forms this binder, and this agrees with the conclusion of Siddique and Mehta [25].

The SEM micrographs of WOC have shown a little porous on the surface and a small scale of possible micro-cracks. It has been noticed an amount of C-S-H gel appears to have decomposed into finer particles and remains of calcium hydroxide crystals. The test has also shown an appearance of small round particles as unreacted cement and a sign of feldspar covering the surface area, which correlates in a positive way with the strength behaviour under compression, as shown in Figure 7.

It becomes difficult to fill the inter-granular space between the grains when the ceramic material is added to the mixture. Therefore, the addition of the spherical particles (ceramic waste) can work as a lubricant, reducing the inside friction among the grain. In addition, it was detected by Senff et al. [26] Due to orientation and settlement, the packing of particles formed from spherical grain is superior to the isotropic structure.

The experiment results have shown an improvement in the internal microstructure of cement paste due to the addition of ceramic material, which acts as a promoter and filler amid hydration of pozzolanic and cement with free C-H. Moreover, the WOC samples have revealed a more uniform and filled structure in comparison to PC. It is noteworthy that C-S-H gel improved in the form of a 'stand-alone' cluster, joined together with needle hydrates because of the deposition of $Ca(OH)_2$ crystal, which extends in the OPC paste. Likewise, a dense and compacted structure was shown in the microstructure of cement pastes containing ceramic waste that fills fine pores. The $Ca(OH)_2$ or C-H crystal has been reduced due to the ceramic cement pozzolanic action with free portlandite to produce new C-S-H.

Nanoparticles were observed in the concrete to perform as an activator and accelerate the cement hydration process. They also perform as an important part of cement paste during the formation of the size of $Ca(OH)_2$ crystal. The SEM micrographs show some ceramic particles readily react with C-H to produce a new form of C-S-H, enhancing the concrete strength. The SEM micrographs have shown a black and white mass which is C-S-H gel spread on the aggregate and performed as a binder in concrete. All mixes have needle hydrates, but the degree of crystallisation varies from mix to mix.

The surface of basalt fiber before mixing into concrete was smooth as presented in Figure 8; while cracks were observed on the surface of fiber after mixing into concrete. The embedded fiber in the hybrid mix indicated the proper bonding of PVA-CR fiber with that matrix as evident from Figure 8. The proper bond between matrix and PVA-CR fiber in hybrid fiber specimens bridge across the cracks and significantly enhanced the strength of hybrid concrete more than that of respective plain concrete as mentioned in the previous section. Figure 8 demonstrates the fiber breakage and surface damage (skin of fiber peeled off) of PVA fiber. The basalt fiber bridge across the cracks and fiber breakage was occurred due to the crack propagation that split the fiber into two parts and the surface damage was because of frictional forces between fiber and matrix during applied load. The cracks in the mix after fiber pull out and fracture of PVA-CR fiber after exposure to high temperature are illustrated in Figure 8. However, after fracturing of PVA-CR fiber due to pull out it was observed that the cement hydration products were attached on the surface which indicated the proper bond of fiber with composite ultimately resulted in higher energy consumption under applied load. On the other hand, it might be noted that still the hydration products are attached to that fiber surface which could be the cause of improved strength of all hybrid fiber composites as compared to that of respective plain concrete. Thus, the soptimised dosage of fiber in composites would play a positive role in the enhancement of mechanical performance than that of plain and ceramic concrete specimens.

Energy-dispersive spectroscopy (EDS) was used to investigate the microchemistry of the selected samples. It has been used to obtain a localised chemical analysis using an X-ray spectrum emitted through a solid sample bombarded with electrons focused beam.

When using the X-rays, distinct positions along the line are detected, while the SEM electron rays scan across the specimen along a predetermined line across the specimen. A detailed analysis of the X-ray energy spectrum is provided at each position.A plot of the relative elemental concentration along the line for each element versus is obtained. The elemental weight of the PC and WOC specimens is shown in Figures 8 & 9. The detected main elements of PC concrete are C, O, F, Mg, Al, Si, Ca, Fe and C, O, F, Mg, Al, Si, S, K, Ca, Ti, Fe, Zr, Au for WOC concrete as sown in the Tables 7, 8 and 9.

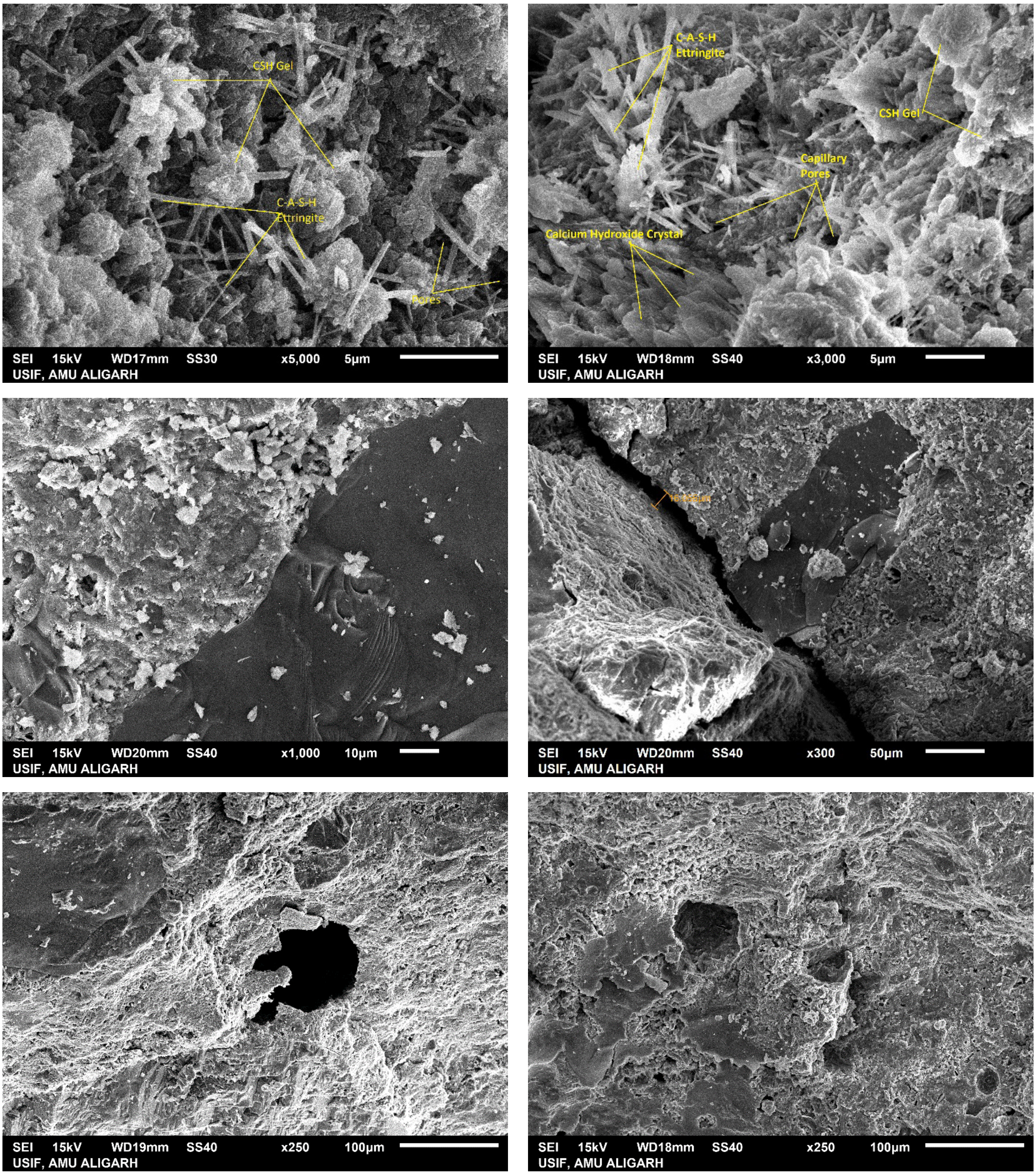

Figure 6. SEM of PC Concrete

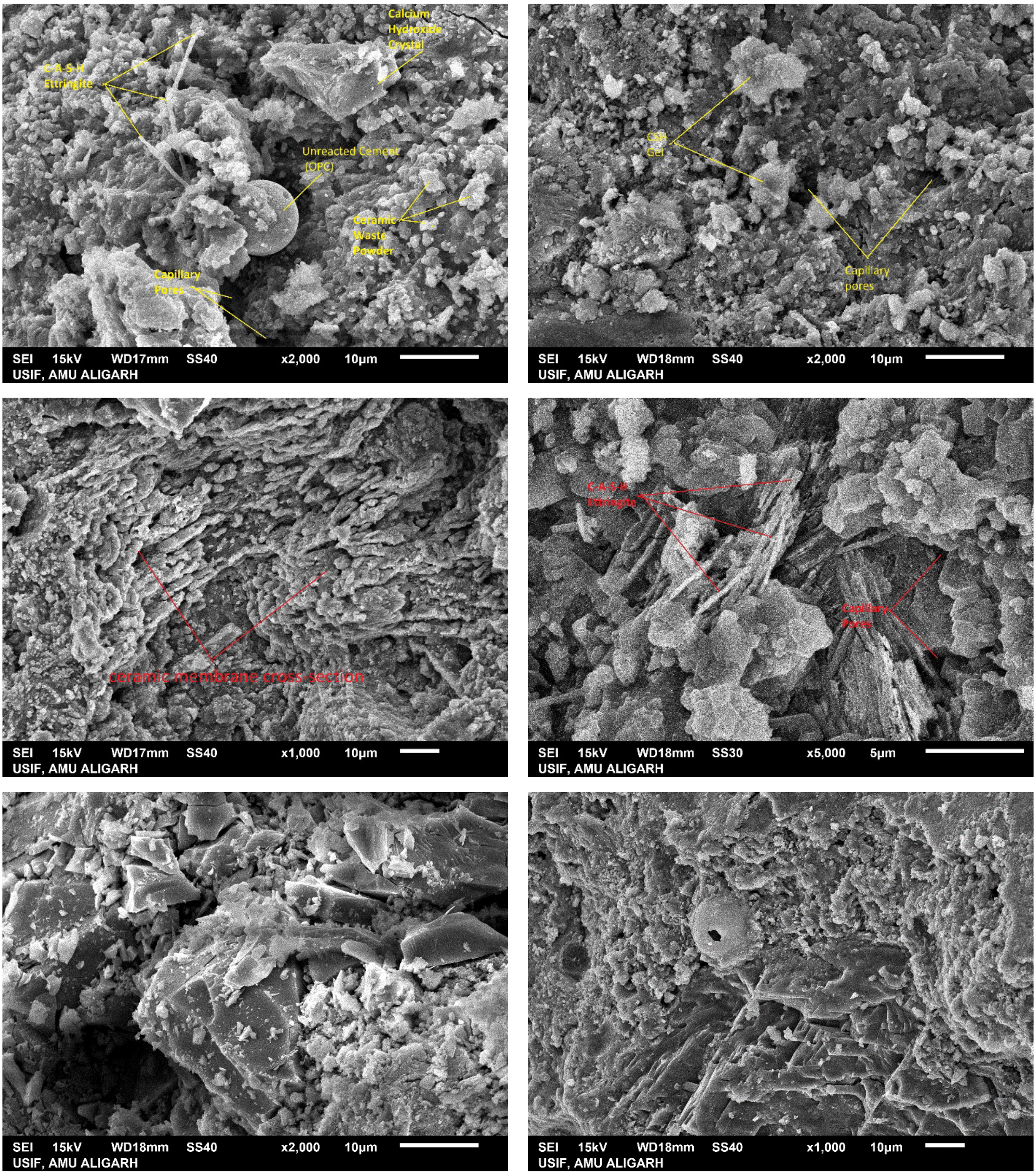

Figure 7. SEM of WOC Concrete

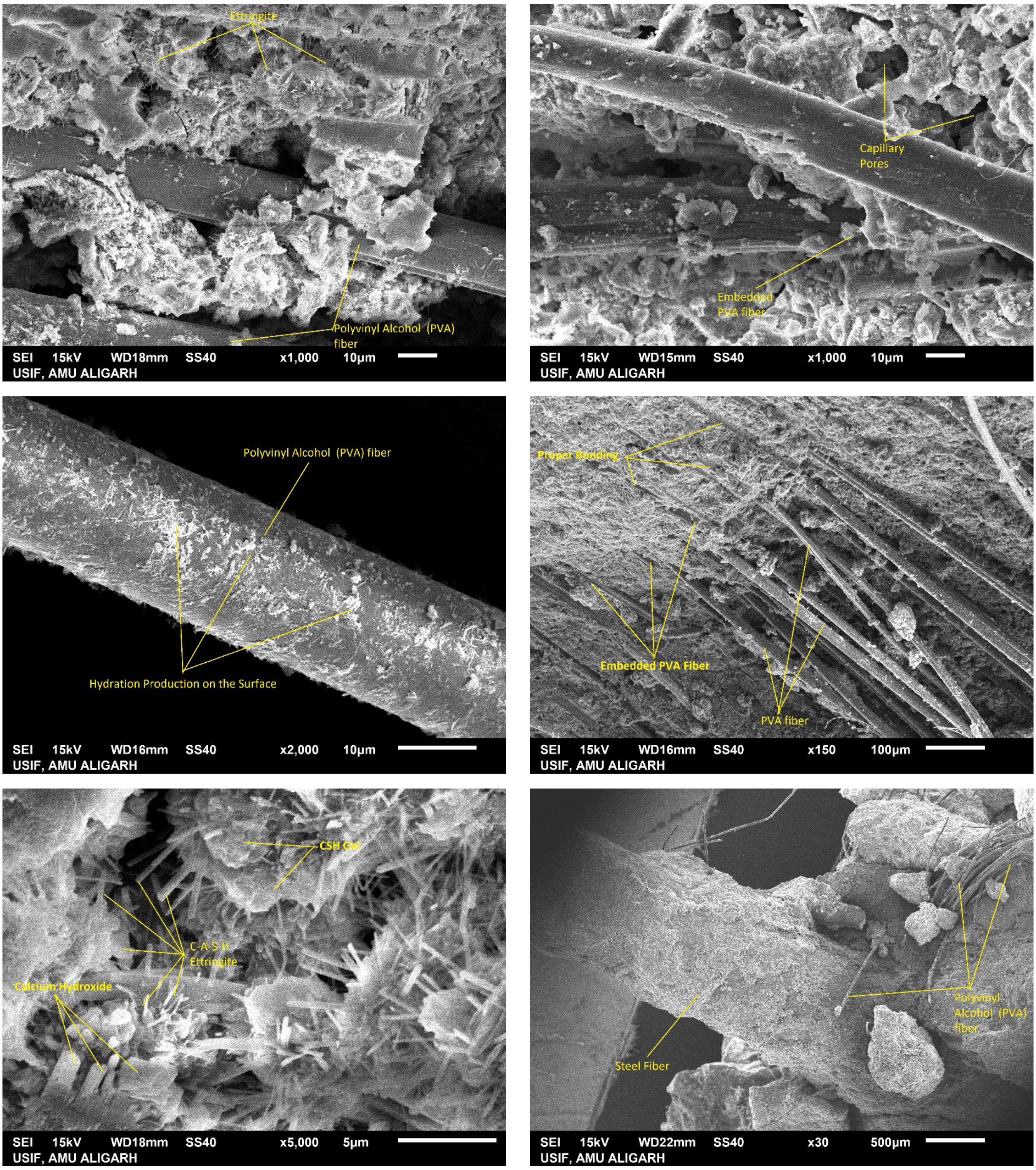

Figure 8. SEM of WOC-Hybrid Concrete

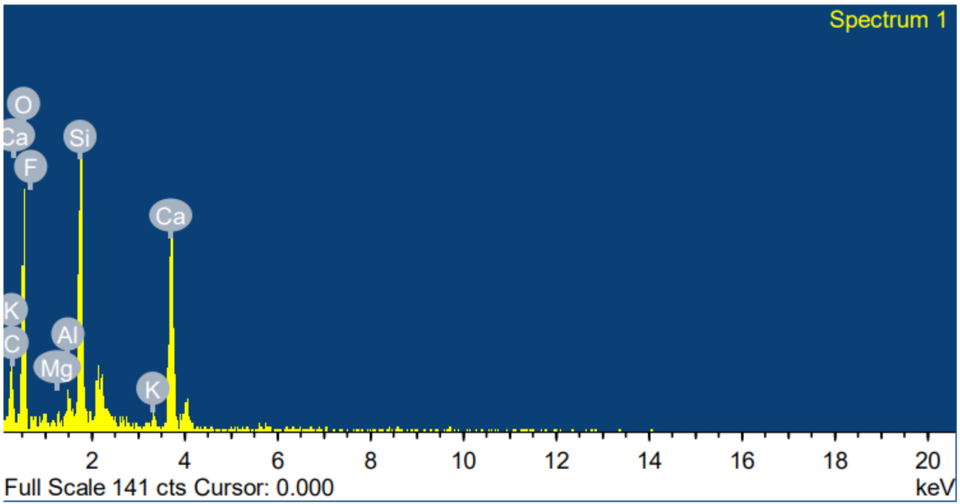

(a)

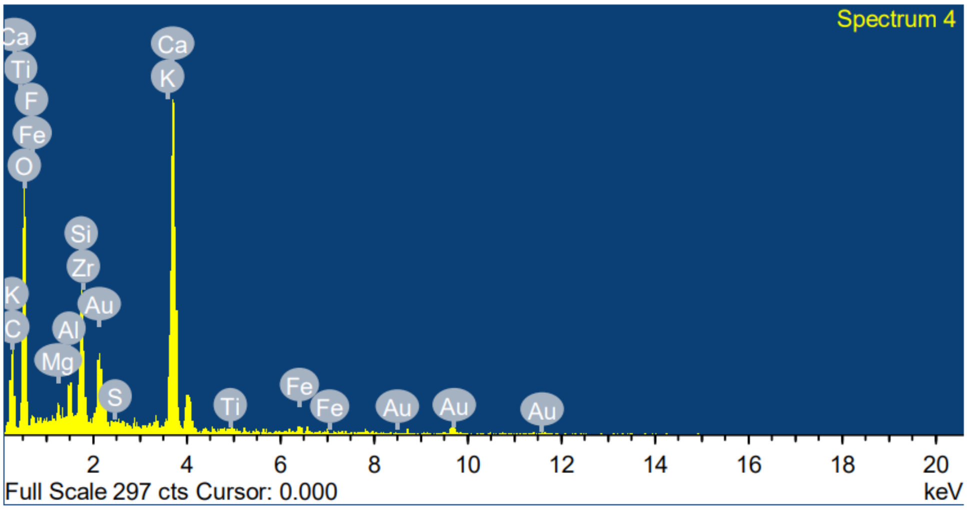

(b)

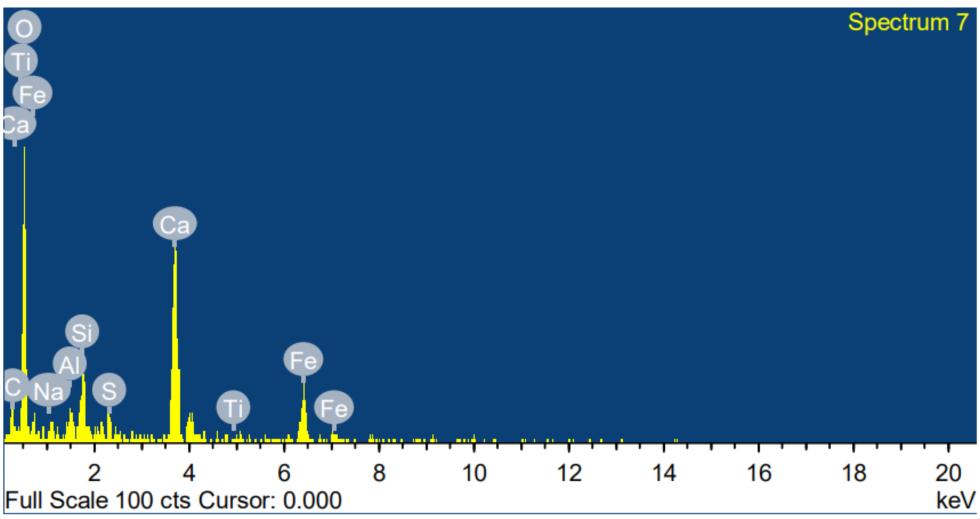

(c)

Figure 9. SEM of: a) PC, b) WOC and c) WOC-Hybrid element Concrete

Table 7. PC element

Standard	Element	Weight%	Atomic%
$CaCO_3$	C	8.77	14.26
SiO_2	O	52.67	64.29
MgF_2	F	0.9	0.73
MgO	Mg	0.60	0.47
Al_2O_3	Al	2.05	1.48
SiO_2	Si	9.56	6.64
Wollastonite	Ca	25.41	12.38
Fe	Fe	0.64	0.22
	Totals	100.00	

Table 8. WOC element

Standard	Element	Weight%	Atomic%
$CaCO_3$	C	8.12	13.64
SiO_2	O	51.72	65.27
MgF_2	F	5.36	5.69
MgO	Mg	0.48	0.4
Al_2O_3	Al	1.43	1.07
SiO_2	Si	3.97	2.85
FeS2	S	0.2	0.12
K	MAD-10 Feldspar	0.57	0.29
Ca	Wollastonite	25.41	12.38
Ti	Ti	0.03	0.01
Fe	Fe	0.56	0.2
Zr	Zr	0.4	0.09
Au	Au	8.33	0.85
	Totals	100.00	

Table 9. WOC-Hybrid element

Standard	Element	Weight%	Atomic%
$CaCO_3$	C	9.05	14.23
SiO_2	O	60.71	71.62
Albite	Na	0.98	0.8
Al_2O_3	Al	0.98	0.69
SiO_2	Si	2.62	1.76
FeS2	S	1.51	0.89
Ca	Wollastonite	13.97	6.58
Ti	Ti	0.10	0.04
Fe	Fe	10.07	3.4
	Totals	100.00	

5. Conclusions

The present study investigated the compressive, tensile, flexural and combined (flexural and torsional) strength of concrete made of hybrid fibers (Steel + PVA). The following conclusions can be drawn:

- Based on the present experimental investigations, hybrid fiber concrete offers several characteristics that cannot be achieved with a single fiber type. Besides, a balance of costs and performance with hybrid composites can be achieved.
- In CS tests, the CS of WOC concrete has increased with the addition of hybrid fibers (CR or HK and PVA). The specimens of PVA-HK-WOC have shown the highest CS values enhancement up to 21.73%. These results are attributed to stronger hydrogen bonding by the hydrophilic PVA fiber, which led to superior resistance to crack propagation and microcracking. For this reason, the increase in compressive strength of concrete reinforced with PVA fiber and hook-ended steel fiber is larger than concrete reinforced with single steel fiber. The specimens of PVA-CR-WOC have shown an enhancement in CS values up to 16.87%.
- In TS tests, TS of WOC concrete increased with the addition of hybrid fibers (CR or HK and PVA). The specimens of PVA-CR-WOC have shown an enhancement in TS value up to 85.44%. Whereas the specimens of PVA-HK-WOC have shown an enhancement in TS values up to 55.97%. This is because the steel fiber is stiffer and stronger than PVA and provides ultimate strength and adequate first crack strength. In contrast, the PVA fiber is relatively flexible and provides improved toughness and strain capacity in the post-crack zone.
- In FS tests, FS of WOC concrete increased with the addition of hybrid fibers (CR or HK and PVA). The specimens of PVA-CR-WOC have shown the highest FS value up to 70.73%. Whereas the specimens of PVA-HK-WOC showed enhancement in FS values up to 48.14%. This result is attributed the PVA fibers effectively controlling the crack propagation at the bending crack tip. The steel fibers resist the widening of the crack width, thereby greatly enhancing concrete's flexural strength.
- In FTS test, the UBS of WOC increased with the addition of hybrid fibers (CR or HK and PVA). The specimens of PVA-CR-WOC and PVA-HK-WOC have shown a great enhancement in UBS values under torsion 243 N.mm, 254 N.mm, 265 N.mm up to 77.78%, 91.66% and 81.81%; 55.55%, 50% and 45.45% respectively.

Funding

No funding was received for conducting this study.

Financial Interests

The authors declare they have no financial interests.

Conflicts of Interests

All authors certify that they have no affiliations with or involvement in any organisation or entity with any financial interest or non-financial interest in the subject matter or materials discussed in this manuscript.

References

[1] Yang, K.H., 2010. Slump and mechanical properties of hybrid steel-PVA fiber reinforced concrete. Journal of the Korea Concrete Institute. 22(5), 651-658. DOI: https://doi.org/10.4334/JKCI.2010.22.5.651

[2] Banthia, N., Soleimani, S.M., 2005. Flexural response of hybrid fiber-reinforced cementitious composites. ACI Materials Journal. 102(6), 382.

[3] Najm, H.M., Ahmad, S., 2021. The effect of metallic and non-metallic fiber on the mechanical properties of waste ceramic concrete. Innovative Infrastructure Solutions. 6(4), 1-15. DOI: https://doi.org/10.1007/s41062-021-00571-4

[4] Keshavarz, Z., Mostofinejad, D., 2019. Porcelain and red ceramic wastes used as replacements for coarse aggregate in concrete. Construction and Building Materials. 195, 218-230. DOI: https://doi.org/10.1016/j.conbuildmat.2018.11.033

[5] Heidari, A., Tavakoli, D., 2013. A study of the mechanical properties of ground ceramic powder concrete incorporating nano-SiO_2 particles. Construction and Building Materials. 38, 255-264. DOI: https://doi.org/10.1016/j.conbuildmat.2012.07.110

[6] Torkittikul, P., Chaipanich, A., 2010. Utilisation of ceramic waste as fine aggregate within Portland cement and fly ash concretes. Cement and Concrete Composites. 32(6), 440-449. DOI: https://doi.org/10.1016/j.cemconcomp.2010.02.004

[7] Awoyera, P.O., Ndambuki, J.M., Akinmusuru, J.O., et al., 2018. Characterisation of ceramic waste aggregate concrete. HBRC Journal. 14(3), 282-287. DOI: https://doi.org/10.1016/j.hbrcj.2016.11.003

[8] Yoo, D.Y., Banthia, N., 2017. Experimental and numerical analysis of the flexural response of amorphous metallic fiber reinforced concrete. Materials and Structures. 50(1), 1-14. DOI: https://doi.org/10.1617/s11527-016-0899-0

[9] Hannawi, K., Bian, H., Prince-Agbodjan, W., et al., 2016. Effect of different types of fibers on the microstructure and the mechanical behavior of ultra-high-performance fiber-reinforced concretes. Composites Part B: Engineering. 86, 214-220. DOI: https://doi.org/10.1016/j.compositesb.2015.09.059

[10] Bolat, H., Şimşek, O., Çullu, M., et al., 2014. The effects of macro synthetic fiber reinforcement use on physical and mechanical properties of concrete. Composites Part B: Engineering. 61, 191-198. DOI: https://doi.org/10.1016/j.compositesb.2014.01.043

[11] Acikbas, G., Yaman, B., 2019. Wear response of glass fiber and ceramic tile-reinforced hybrid epoxy matrix composites. Iranian Polymer Journal. 28(1), 21-29. DOI: https://doi.org/10.1007/s13726-018-0675-9

[12] Yang, K.H., 2011. Tests on concrete reinforced with hybrid or monolithic steel and polyvinyl alcohol fibers. ACI Materials Journal. 108(6), 664.

[13] Tabatabaeian, M., Khaloo, A., Joshaghani, A., et al., 2017. Experimental investigation on effects of hybrid fibers on rheological, mechanical, and durability properties of high-strength SCC. Construction and Building Materials. 147, 497-509. DOI: https://doi.org/10.1016/j.conbuildmat.2017.04.181

[14] Kim, D.H., Park, C.G., 2013. Strength, permeability, and durability of hybrid fiber□reinforced concrete containing styrene butadiene latex. Journal of Applied Polymer Science. 129(3), 1499-1505. DOI: https://doi.org/10.1002/app.38861

[15] Ahlberg, S., Antonopulos, A., Diendorf, J., et al., 2014. PVP-coated, negatively charged silver nanoparticles: A multi-center study of their physicochemical characteristics, cell culture and in vivo experiments. Beilstein Journal of Nanotechnology. 5(1), 1944-1965. DOI: https://doi.org/10.3762/bjnano.5.205

[16] Beaudoin, J.J., 1990. Handbook of fiber-reinforced concrete. Principles, properties, developments and applications. http://worldcat.org/isbn/0815512368.

[17] Najm, H.M., Nanayakkara, O., Sabri, M.M.S., 2022. Destructive and Non-Destructive Evaluation of Fibre-Reinforced Concrete: A Comprehensive Study of Mechanical Properties. Materials. 15(13), 4432. DOI: https://doi.org/10.3390/ma15134432

[18] Najm, H.M., Ahmad, S., Submitter, Y., 2021. Artificial Neural Networks for Evaluation & Prediction of the Mechanical Properties of Waste Ceramic Optimal Concrete Exposed to Elevated Temperature. Available at SSRN 4032028. DOI: http://dx.doi.org/10.2139/ssrn.4032028

[19] Nanayakkara, O., Najm, H.M., Sabri, M.M.S., 2022. Effect of Using Steel Bar Reinforcement on Concrete Quality by Ultrasonic Pulse Velocity Measurements. Materials. 15(13), 4565.
DOI: https://doi.org/10.3390/ma15134565

[20] Najm, H.M., 2022. Utilisation of Hybrid Fibers for Sustainable Concrete Production -A Review of Mechanical Properties. International Journal of Engineering and Manufacturing (Under Review).

[21] IS 10262-, 2009. Indian Standard Concrete Mix Proportioning – Guidelines, Bureau of Indian Standards, New Delhi 110002.

[22] Mohammed, H., Ahmed, S., 2020. Mechanical Performance Evaluation of Concrete with Waste Coarse Ceramic Aggregate. Smart Cities—Opportunities and Challenges (pp. 593-605). Springer, Singapore.
DOI: https://doi.org/10.1007/978-981-15-2545-2_49

[23] Najm, H.M., Ahmad, S., 2022. The Use of Waste Ceramic Concrete for a Cleaner and Sustainable Environment-A Comprehensive Study of Mechanical and Microstructural Properties. Civil Engineering and Environmental Report. (In press).

[24] Najm, H.M., Ahmad, S., 2021. Effect of elevated temperatures exposure on the mechanical properties of waste ceramic concrete reinforced with hybrid fibers materials. Sigma Journal of Engineering and Natural Sciences. (In press)

[25] Siddique, R., Mehta, A., 2014. Effect of carbon nanotubes on properties of cement mortars. Construction and Building Materials. 50, 116-129.

[26] Senff, L., Hotza, D., Repette, W.L., et al., 2010. Effect of nanosilica and microsilica on microstructure and hardened properties of cement pastes and mortars. Advances in Applied Ceramics. 109(2), 104-110.

Journal of Architectural Environment & Structural Engineering Research
https://ojs.bilpublishing.com/index.php/jaeser

ARTICLE

3D Simulation of Battery Fire on a Large Steel Frame Structure due to Depleted Battery Piles

Nicole Braxtan[1] Jorge Nunez[1] Shen-En Chen[1*] Tiefu Zhao[2] Lynn Harris[3] Dave Cook[4]

1. Department of Civil and Environmental Engineering, University of North Carolina at Charlotte, Charlotte, NC 28223, US
2. Department of Electrical and Computer Engineering, University of North Carolina at Charlotte, Charlotte, NC 28223, US
3. Deutsche Bahn, Raleigh, NC, US
4. Rail Propulsion Systems, Fullerton, CA, US

ARTICLE INFO

Article history
Received: 23 August 2022
Revised: 25 September 2022
Accepted: 11 October 2022
Published Online: 12 October 2022

Keywords:
Lithium ion battery
Train fire
Propagation
Structural safety

ABSTRACT

Lithium ion batteries (LIB) can rupture and result in thermal runaway and battery fires. In the process of transporting lithium ion batteries using trains, the massive collection of batteries can cause train fire and pose significant danger to the public. This is especially critical when the fire occurs amid a heavily populated metropolitan environment. This paper reports the 3D analysis of a warehouse with possible train fire due to LIB rupture and the fire propagation at a rail yard. Six critical fire cases with the battery train in close vicinity to the warehouse were considered. The six fire cases are the worst-case scenarios of a Monte Carlo simulation of different fire cases that may occur to an actual steel storage facility at the Capital Railyard, Raleigh, North Carolina. A 3D finite element (FE) frame model was constructed for the steel warehouse and the most critical fire cases were simulated. The results indicated that several structural components of the warehouse would experience large stresses and deflections during the simulated battery fires and resulting in instability to the structure. Specifically, members of the roof frame represent the most critical elements and that the members can result in large deformations as early as 4 minutes after the fire starts. Furthermore, effective utilization of fire protection can delay somewhat the fire effects and extend time to failure to 45 minutes and in one of the simulated cases, prevent structural instability. Thus, fire from LIB waste transport using train is a very realistic problem due to the thermal runaway, and the analysis performed in current study can be used as a preventive investigation technique for buildings that may be exposed to the train fire risk.

*Corresponding Author:
Shen-En Chen,
Department of Civil and Environmental Engineering, University of North Carolina at Charlotte, Charlotte, NC 28223, US;
Email: schen12@uncc.edu

DOI: https://doi.org/10.30564/jaeser.v5i3.4985

1. Introduction

Li-ion battery (LIB) is currently the energy storage/use technology of choice due to its high energy density and the capability for rapid energy draw [1]. To date, significant amounts of LIBs have been manufactured and used, and the disposal of LIBs is now a critical environmental and safety issue [2]. The disposal of LIBs usually involves transporting them in bulks to either recycling centers where physical separations are performed or straight to landfills [3]. In the US, fire safety of commercial LIBs has been addressed by federal regulations (Federal Register, 2007, 49 CFR parts 171, 172, 173 and 175) [4]. However, no specific guidelines on the transport of spent Li-ion batteries can be found.

Fire impacts due to battery stockpile explosions were raised when in 2017, a double decker rail cargo car carrying lithium ion waste batteries caught fire and exploded in downtown Houston [5]. The incident damaged several residential structures due to the blast shock waves [6]. LIB fires are known to induce damages to nearby structures [7]. The Houston incident instigated the potential danger of fire during mass transport of depleted lithium-ion batteries. In the case of the Houston incident, the fire was propagated to the surrounding area and resulted in nearly an acre of burnt grass field. Figure 1 shows the correlation between battery fire to full-scale locomotive fire as in the case of the Houston train. The inserted curve shows the time history of a single battery cell fire that can rise to maximum temperature in a very short time.

Studies on lithium ion battery fire are limited and design guidelines to prevent fire damage due to lithium ion battery fire are almost non-existent. Thermal runaway, in particular, is one of the failure modes in batteries and distinguishes Lit-ion battery fire from other vehicle fires. For the LIB, thermal runaway is caused by exothermic reactions between the electrolyte, anode, and cathode – with temperature and pressure increasing in the battery, the reaction rate increases due to a temperature increase causing further increases in temperature and hence a further increase in the reaction rate. Eventually, the battery will rupture and may result in an explosion or fire [8,9].

Figure 2 shows the schematic of an operating LIB where electricity is generated when the electrolyte causes chemical changes between the cathode (lithium metal) and the anode (carbon). A thermal runaway (Figure 2b) occurs when the battery experiences a change and several things could happen at the same time: Heating can start, resulting in the breakdown of protective layers and electrolytes, releasing flammable (toxic) gas, resulting in the melting of the separator and leading to short circuit. Finally, the cathode breaks down and generates oxygen and further forces temperature increase. For bulk storage of lithium-ion batteries, the fire propagation can be initiated by battery pack deformation, such as due to a punch-through [10]. Hence, the packaging design of a battery pack plays an important role in preventing cell fire propagation [11].

Thermal runaway is different from conventional fire in that it is fueled by internal exothermic reactions and the supply of oxygen is not essential to the continuation of the chemical process. As a result, the conventional fire extinguishing technique of removing oxygen will not work for LIB thermal runaway. Furthermore, LIB stack fire may result in explosions and the emission of toxic gases, this is evident in the April 19, 2019 battery fire of the AES battery energy storage (BESS) facility in Arizona [12].

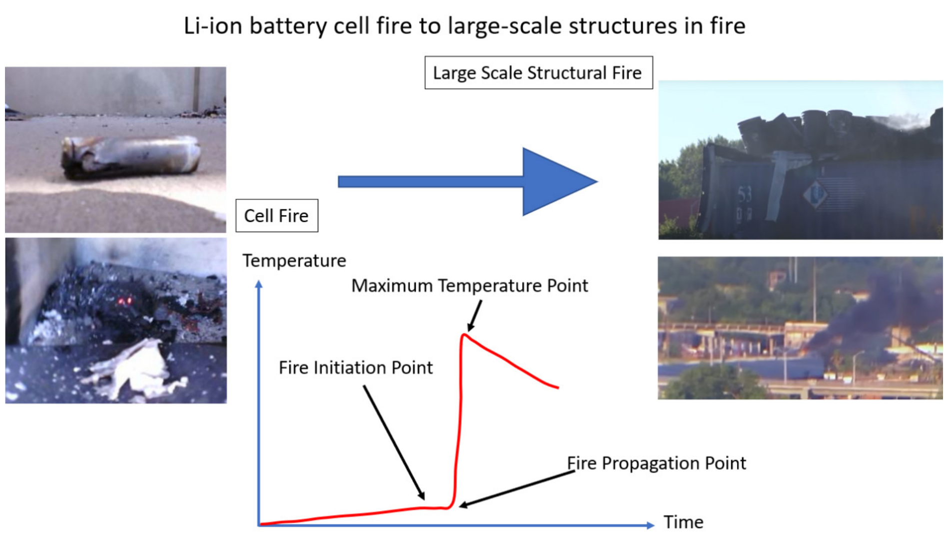

Figure 1. Train Fire due to Battery Cell Thermal Runaway

A review of fire on trains showed that train fire investigation and prevention have been addressed in several publications from the APTA (American Public Transportation Association), including the APTA Recommended Practice for Transit Bus Fire/Thermal Incident Investigation for fire safety analysis of existing passenger rail equipment [13], recommended practices for fire safety [14], for fire protection systems [15], fire safety analysis for existing passenger rail equipment [16] and fire detection technologies [17]. Although these guidelines are not directly related to LIB safety, they can be modified to address fire from Li-ion batteries.

Other fire protection recommendations can be found in publications from the National Fire Protection Association (NFPA) including NFPA 130 [18] which specifically addresses fire protection. For general building structure fire protections, guidelines that may be applicable include the International Building Code [19], which defines fire resistance ratings for buildings based on construction type and building element.

In summary, to ensure fire safety, a fire risk analysis needs to be performed for potential at-risk buildings. The fire risk analysis should result in the identification of the most critical risk scenarios for the safety design of the structure [20]. Detailed structural analysis can then be performed to understand the responses of the structure to the fire risk. To demonstrate a fire risk analysis, this paper describes a fire evaluation performed on an existing steel metal structure with close-by railroads that may be exposed to battery train fires.

In order to assess the responses of the steel frame structure from the worst fire risk case, a nonlinear finite element (FE) fire analysis is conducted based on the most likely fire scenarios from the established fire cases. The worst-case scenarios are established based on a Monte Carlo simulation (fire risk analysis) of more than 5,000 fire cases performed using Cellular Automata. The analysis identified six most critical fire cases. In order to identify the most vulnerable fire propagation event to the structural members, a 3D frame structure model is developed to analyze the steel frame structure which is shown in Figure 3. The most critical fire cases (fire propagating to specific building compartments), derived from the fire risk analysis, were then simulated using the FE model. The 3D analysis allowed a realistic simulation of the fire scenarios and helped indicate the most critical locations for the selected fire scenario. The analysis included steel elements idealized both with and without fire protections to the structure. The analysis process presented in this paper is holistic and consider all likely fire scenarios for the steel frame structure and can be used for any other structures that may be exposed to risks from a LIB fire.

1.1 North Carolina Capital Railyard Warehouse

The steel frame structure is a train repair warehouse at the North Carolina Department of Transportation (NCDOT) Capital Yard in Raleigh, North Carolina. The open-span steel frame structure has metal sidings and roofs and is used for sheltered repair and maintenance works for the Piedmont Railroad serving cities between Raleigh and Charlotte, North Carolina. Two railroad tracks run close (within meters) to the building and a very short track dead-ended partially into the building. The tracks dictated the possible parked positions of a train carrying LIB stockpiles.

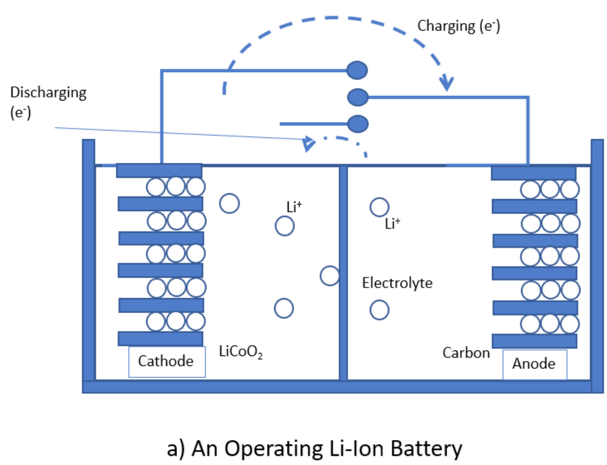

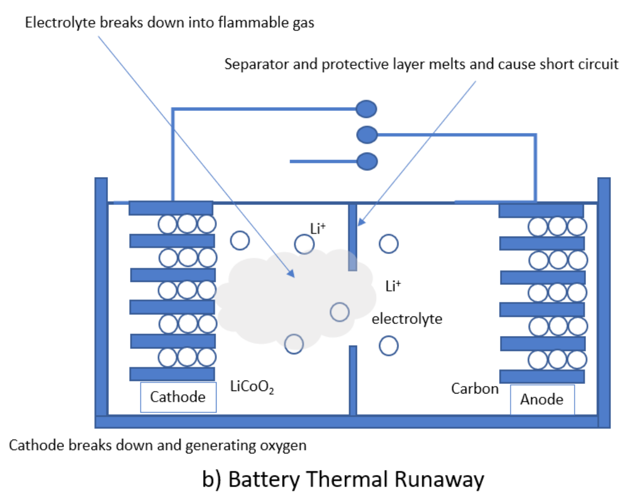

Figure 2. The Li-Ion Battery: a) an Operating LIB cell; and b) LIB Thermal Runaway

a) Exterior of Warehouse

b) Interior of Warehouse

Figure 3. The NCDOT Capital Yard Maintenance Warehouse: a) Exterior and b) interior

The eave height of the warehouse is 7.3 m and the roof is at 9.3 m from the floor slab. Figure 3 shows the steel structure that sits within the NCDOT Capital Yard. The bay width for the floor plan is 7.3 m by 7.9 m. The building is composed of six rigid frames connected with beams and purlins on each roof side between the rigid frames [21-23]. The rigid frame is composed of tapered beams of W18x40's [24]. The purlins are made of C10x25 beams. Figure 4 shows laser scans of the interior of the warehouse. Figure 4a shows the entrance for the train into the building. Figure 4b shows the roofing details of the warehouse. The left side of Figure 4b shows a standalone office structure within the warehouse that was not considered in the numerical modeling. Figure 5 shows the plain view of the original CAD drawing of the building.

Due to the close vicinity of the railroad tracks to the building, hazard arises in that a train filled with disposed LIBs, or a train powered by LIB (hybrid or fully electric), may be parked too close to the structure and potential train fire may propagate to the structure. Hence, a study on the LIB fire risks and the effect of fire on the structure has been performed. The study evaluated the building structure for fire using finite element modeling and a fire risk analysis using an expert opinion approach to establish the risk indices for different fire scenarios, so that the most critical aspects of the building fire can be unpacked for better understanding.

a)

b)

Figure 4. LiDAR Scans of the NCDOT Capital Yard Maintenance Warehouse: a) LiDAR Scan of Warehouse Interior and b) LiDAR Scan of Warehouse Roofing System

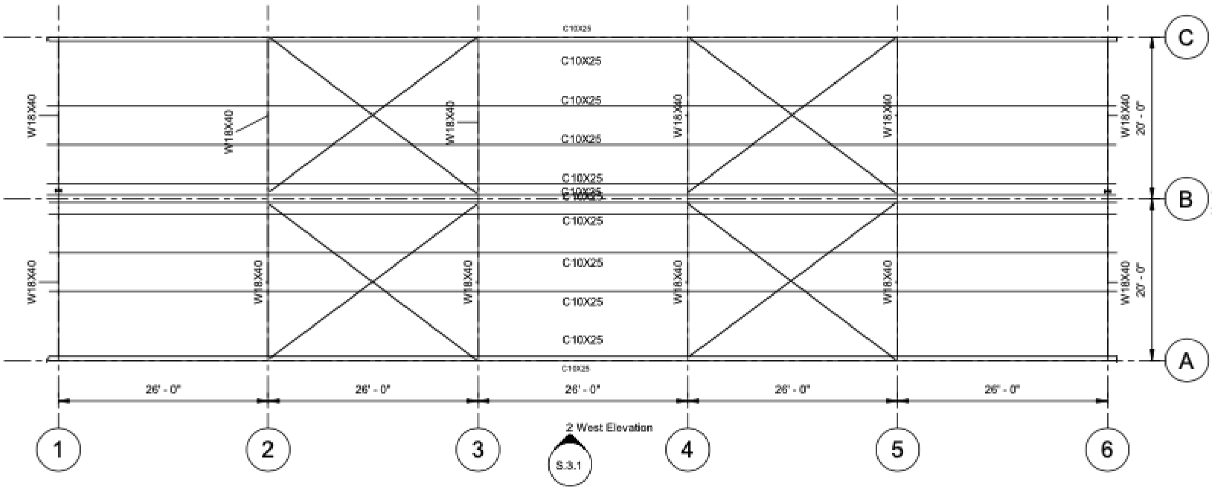

Figure 5. Plan View; Train Warehouse [25]

1.2 Summary of Fire Risk Analysis

The fire risk analysis is conducted using a combination of event probability and severity (risk level), to create a risk rating for a particular event. The probability is scaled from 1 to 5, 1 being frequent and 5 being improbable to occur. The severity aspect is scaled from 1 to 4 where 1 being catastrophic and 4 being negligible. The risk indexing can help prioritize the fire risks, which dictates the structural fire evaluation for the building [25].

The warehouse that is being analyzed in this case study contains fuel, oxygen, and heat source, which are three elements needed in order to ignite a fire. Fire behavior is dependent on the fire temperature, the heat transferred to the surface of the structure, and the corresponding rise of temperature occurring within the structure. Because the warehouse has open space and possible workers within, fire safety will be provided based on the life safety of occupants by identifying the potential fire source and select the best way to control and extinguish the fire at an early stage, and possible extend the time needed for the safe egress of people.

Mira et al. [25] conducted a detailed fire risk analysis wherein the warehouse building was partitioned into 14 exterior and interior compartments, as shown in Figure 6 and described in Table 1. Special considerations for compartments are also included in Table 1 as necessary, dictating additional parameters in the fire ignition and spread potential as well as increased life safety. Current study extends the 2D analysis into 3D and further improve the models to allow the identification of the specific failing members.

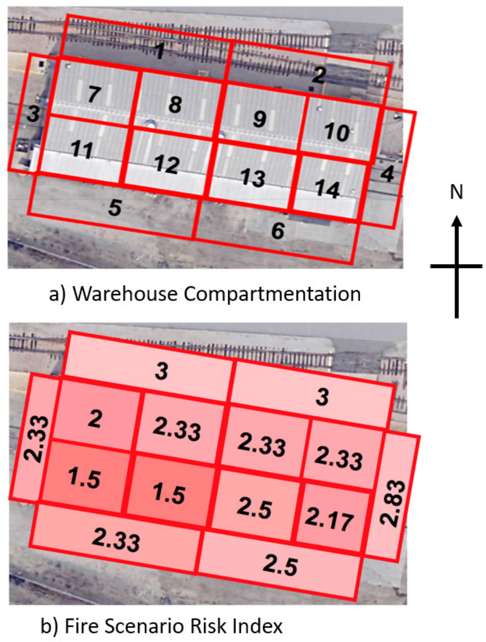

Figure 6. Warehouse Building Compartment Designation [25]

All likely critical elements that may cause fire ignition and spread to the building have been considered, including sources related directly to the LIBs onboard the train and other traditional fire hazards surrounding the building. The fire hazards considered are fire initiated from the train, exterior electric power transformers, power supplies within the warehouse, chemical tanks outside of compartment 13 and 14, overhead transformer fire and a large gas tank behind the building. For this investigation, a total of six specific fire scenarios were considered and used for the fire risk analysis. Each scenario is further identified by

Table 1. Compartment Designations in the Fire Risk Evaluation [25]

Compartment No.	Description	Special Considerations
1	Top left exterior wall (Exterior)	Close proximity exterior tracks
2	Top right exterior wall (Exterior)	Close proximity exterior tracks
3	Middle left exterior wall (Exterior)	Tracks enter into warehouse
4	Middle right exterior wall (Exterior)	Tracks do not enter warehouse
5	Bottom left exterior wall (Exterior)	Adjacent chemical storage
6	Bottom right exterior wall (Exterior)	Wide open door
7	Top left interior structural elements (Interior)	Wide open door
8	Middle top left interior structural elements (Interior)	Power tool storage
9	Middle top right interior structural elements (Interior)	Includes stand-alone office with glass frame (additionally occupancy)
10	Top right interior structural elements (Interior)	Houses electric controls on interior wall
11	Bottom left interior structural elements (Interior)	Railroad tracks extend through for sheltered repair work
12	Middle bottom left interior structural elements (Interior)	Railroad tracks extend through for sheltered repair work
13	Middle bottom right interior structural elements (Interior)	Adjacent chemical storage
14	Bottom right interior structural element (Interior)	Adjacent chemical storage

a numeric number and the detailed description for each scenario is shown in Table 2.

A survey was sent out to individuals seeking expert opinions on the fire cases and the ranking of the cases. The risk index matrix was established where each of the six fire scenarios was individually applied to the compartments of the warehouse. The risk analysis resulted in a total of 84 scenarios. The expert opinion approach involved ten expert members and each ranked the risks independently. The average risks from the collected opinions of the seven members were calculated and then used to rank the different scenarios. The most and least critical areas of the warehouse were then identified. The outcomes are then mapped onto the compartment schematic shown in Figure 6, where the lower risk index values mean higher potential fire risks. From Figure 6b), it is shown that the most significant fire scenario is the fire propagating due to battery train parked inside of the structure and train fire propagating to compartments 11 to 12. The least significant fire scenario is when fire occurring to compartments 7, 8, 9 and 10. Hence, detailed structural fire analysis was conducted to compartments 11 to 13. The compartment 13 was included to extend the fire analysis for multiple bays of the structure.

Table 2. Detailed Fire Scenarios [25]

Fire Scenario	Details
(1) Train Fire Outside*	Ignition: Battery thermal runaway in locomotive. Fire development: Easily igniting material catches on fire. Fire propagation: Fire material smolders and propagate to warehouse.
(2) Train Fire Inside*	Ignition: Battery thermal runaway in locomotive. Fire development: Easily igniting material catches on fire. Fire propagation: Fire material smolders and propagate to warehouse.
(3) Chemical Storage Fire**	Ignition: Storage containment unit ignites. Fire development: Flammable material catches on fire. Fire propagation: Fire material smolders and propagate to warehouse.
(4) Power Electronics Fire**	Ignition: Short circuit of poorly insulated power electronics. Fire development: Flammable material catches on fire. Fire propagation: Fire material smolders and raise temperature.
(5) Transformer Fire**	Ignition: Transformer catches fire due to short circuit. Fire development: Easily igniting material catches on fire. Fire propagation: Fire material smolders and propagate to warehouse.
(6) Gas Containment Fire**	Ignition: Gas containment unit catches on fire. Fire development: Easily igniting material catches on fire. Fire propagation: Fire material smolders and propagate to warehouse.

*Fire starting scenarios associated with train with LIBs

*Fire starting scenarios specific to the NCDOT railyard warehouse

2. Structural Fire Analysis

A 3-D structural finite element model was developed using Abaqus Finite Element Software [26] to investigate high-risk fire scenarios present on the rail warehouse structure. A 3-D frame model was constructed as shown in Figure 7, using two-node cubic beam elements (B33) throughout the model, with tapered cross-sections defined on the column elements and fixed support boundary conditions at the base of the frame [27]. Self-weight was applied using a gravity load in addition to a superimposed dead load of 958 Pa. Both self-weight and superimposed dead load were held constant as the fire load was specified through a temperature field [28] applied to the steel members. General static steps with automatic incrementation and nonlinear geometry were used throughout the analysis.

In lieu of a full heat transfer finite element solution, an iterative, transient heat transfer analysis was performed on the unprotected steel members exposed to fire based on the temperature rise of the steel member, ΔT_s defined in the AISC Specifications [24]:

$$\Delta T_s = \frac{a}{c_s\left(\frac{W}{D}\right)}(T_F - T_s)\Delta t \tag{1}$$

where,

a = heat transfer coefficient, Btu/(ft^2-s-^{o}F)(W/m^2-^{o}C)
= $a_c + a_r$

a_c = convective heat transfer coefficient

a_r = radiative heat transfer coefficient, given as:
= $\frac{S_B \varepsilon_F}{T_F - T_s}\left(T_{FK}^4 - T_{SK}^4\right)$

c_s = specific heat of the steel, Btu/lb-^{o}F (J/kg-^{o}C)

D = heat perimeter, in. (m)

S_B = Stefan-Boltzmann Constant = 5.67 x 10^{-8} SWm^{-2}k^{-4}

T_F = temperature of the fire, ^{o}F (^{o}C)

T_{FK} = temperature of the fire, ^{o}K
= (T_S+459)/1.8 for TF in ^{o}F
= (T_S+273) for TF in ^{o}C

T_S = temperature of the steel, ^{o}F (^{o}C)

T_{SK} = temperature of the steel, ^{o}K
= (T_S+459)/1.8 for TF in ^{o}F
= (T_S+273) for TF in ^{o}C

W = weight (mass) per unit length, lb/ft (kg/m)

ε_F = emissivity of the fire and view coefficient

Δt = time interval, s

The hydrocarbon fire was chosen for the design fire for a large-scale lithium-ion battery fire, offering a fire scenario with more rapid temperature rise and higher temperatures than the standard E119 fire typically used for compartment fires with traditional building material fuel loads. Figure 8b compares the hydrocarbon fire and resulting unprotected steel member temperatures to the temperatures specified in the ASTM E119 Standard fire. Additionally, a modified fire curve was developed to simulate steel members with appropriate fire protection applied where the hydrocarbon fire curve was scaled to limit the temperature of the steel members to 538 °C [25]. The emissivity was assumed to be 0.7, typical of steel structures, and a convection coefficient of 50 W/m^{2}K was used for the hydrocarbon fire [30].

Abaqus *Elastic and *Plastic parameters were used to input temperature-dependent, nonlinear material properties for the steel. Temperature-dependent coefficient of thermal expansion was calculated based on the thermal strain defined in Eurocode [29,30] and is shown in Figure 8b. Density was specified as a constant 7,850 kg/m^3.

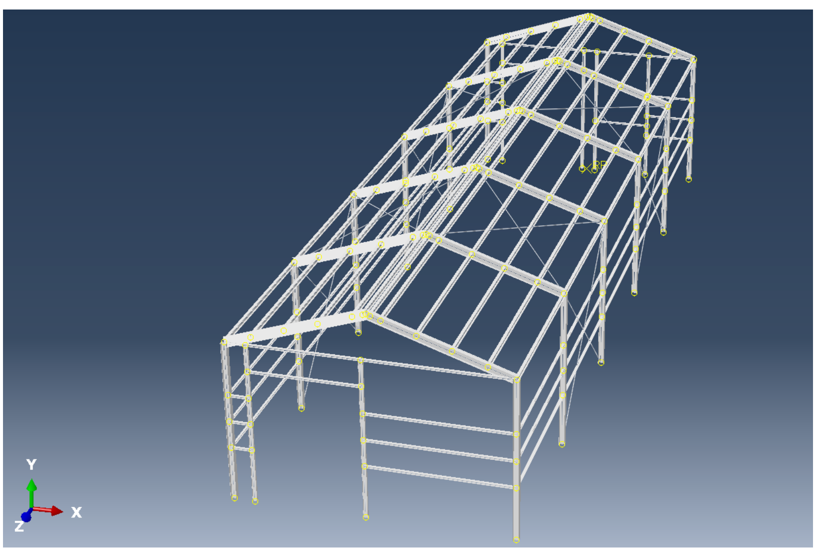

Figure 7. Overall FE Model Geometry

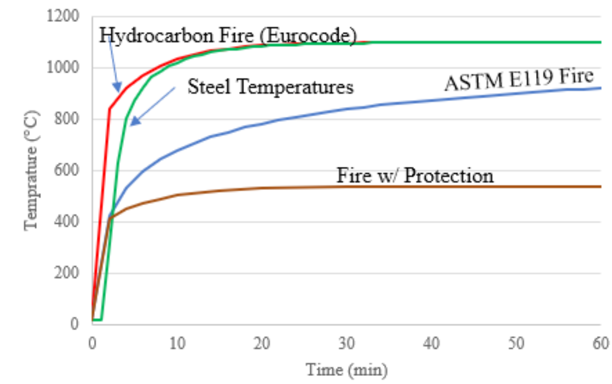

a)

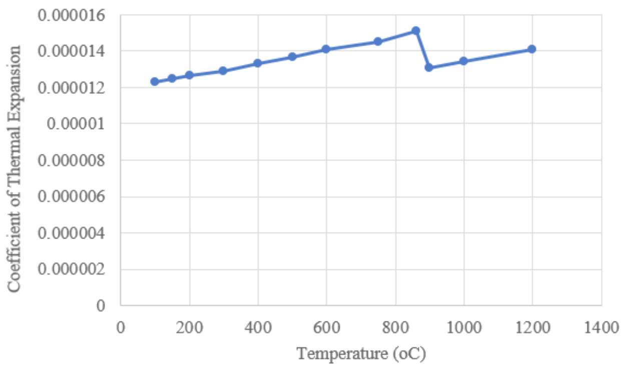

b)

Figure 8. Thermal Characteristics of Fire Used in FE Modeling (a) Fire Curves and Steel Temperatures (b) Temperature Dependent Thermal Expansion [25]

3. Discussion

3.1 Fire Propagation Analysis

Several iterations of FEA models were generated in Abaqus in order to evaluate the warehouse structure under various fire design curves and levels of exposure. The FEA models were based on building dimensions which were generally similar to that of the existing railyard structure, however structural members were modified or replaced to facilitate analysis. The fire design curves used in analysis were limited to the steel temperature fire curve based on heat transfer analysis and the modified fire curve with steel member temperature limited to 538 °C.

The heat transfer analysis curve was assumed to represent steel framing which does not have fire protection and the modified curve was assumed as steel framing with appropriate fire protection. FEA models were identified as "unprotected" and "protected" cases for those consisting of the heat transfer analysis curve and modified fire design curves, respectively, in an effort to create a clear distinction.

As determined by the fire risk analysis, the most significant fire scenarios were related to battery train fire propagating to building compartments. Therefore, FEA models considered the length of a battery train car and the various positions an individual car may occupy within the warehouse. A train car could span anywhere from a single bay in the warehouse up to a total of three bays in length, for which the design fire was first applied to only Bay 11, then Bays 11 and 12, and then Bays 11, 12 and 13. A summary of FEA models is shown in Table 3. As shown in Table 3, the fire protection scenarios are also considered resulting a total of six study cases.

Table 3. FEA Model Summary

Fire Protection	Bays Exposed to Fire	Case
Unprotected (Maximum Design Fire Temperature of 1100 °C)	11	1
	11 and 12	2
	11, 12, and 13	3
Protected (Max Design Fire Temperature of 538 °C)	11	4
	11 and 12	5
	11, 12, and 13	6

The earliest iterations of the Abaqus models were constructed using tapered W18x40 columns along the East and West elevations of the structure, W8x10 columns along the North and South elevations of the structure, W18x40 rafters, C10x25 purlins, and C5x6.7 girts. Analysis of these Abaqus models tended to abort soon after fire was applied to the structural members. The Abaqus software will abort analysis if structural instability is encountered. It was found that these models were improved when wide-flange members were used instead of channels. Therefore, channels were replaced with wide-flange members of a similar section modulus; C10x25 purlins were replaced with W8x21 members and C5x6.7 girts were replaced with W4x13 members.

FE analysis results were obtained from Abaqus in the forms of displacements, Von Mises (Mises) stresses, and temperatures relative to time. Displacements are presented as U1, U2, and U3 which represent deflection in the x, y, and z directions, respectively. Von Mises stresses are presented as SP1, SP5, SP9, and SP13 which is a reference to section points on a cross-section of a wide-flange member as shown in Figure 9. Due to the large amount of data resulting from the analysis, only data from representative nodal points of Purlin and Girt members are included in this paper as these presented the highest levels of stress and deformation. Data for individual nodes for each case are included in Figures 10 through 15. Data for maximum temperature, maximum stress, and maximum absolute deflection for each node is included in Tables 4 through 6, respectively.

In general, for both the Unprotected and Protected design fire cases it was observed that maximum deflection occurs nearly at the same time as the maximum temperature. Also, maximum stress levels occur within the first four minutes of the design fire for both design fire cases. In most cases, it was observed that members reached stress levels between 241.3 MPa (35ksi) and 337.8 MPa (49ksi), which is near yield-stress for most common grades of steel. Only three nodes, of the fourteen nodes observed, have stress recordings below the yield-stress level yet they had maximum deflections between seventeen and twenty-three inches. These three nodes were part of the unprotected design fire cases.

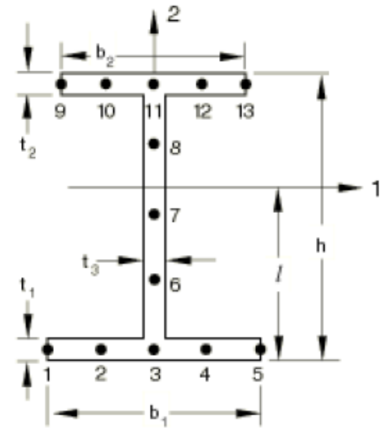

Figure 9. W-Beam Section Points

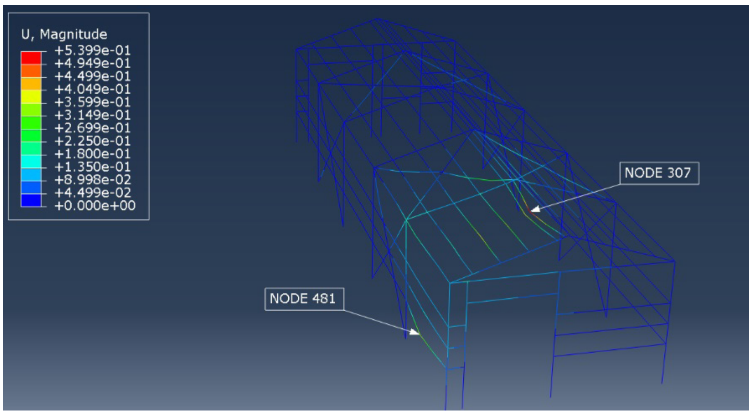

a) Case 1 Node Locations

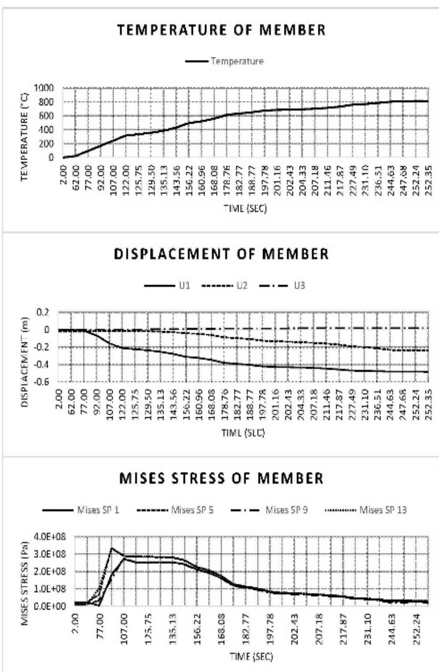

b) Case 1- Purlin Node 307

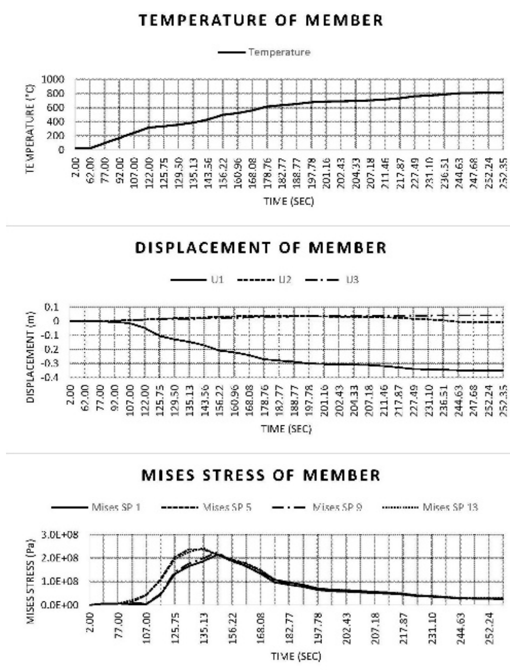

c) Case 1- Girt Node 481

Figure 10. Case 1 Results

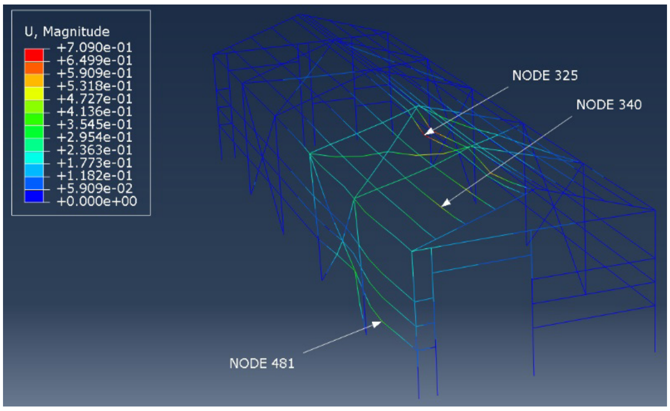

a) Case 2 Node Locations

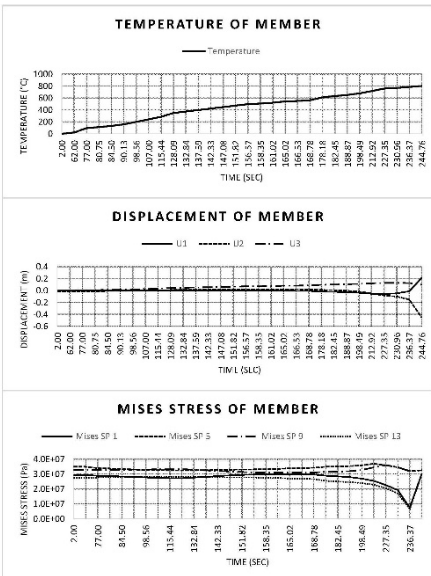

b) Case 2- Purlin Node 325

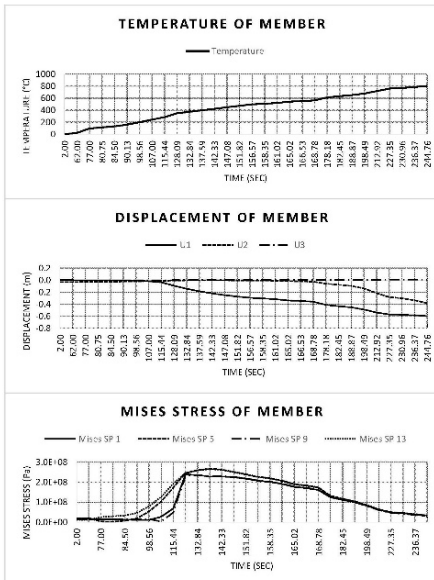

c) Case 2- Purlin Node 340

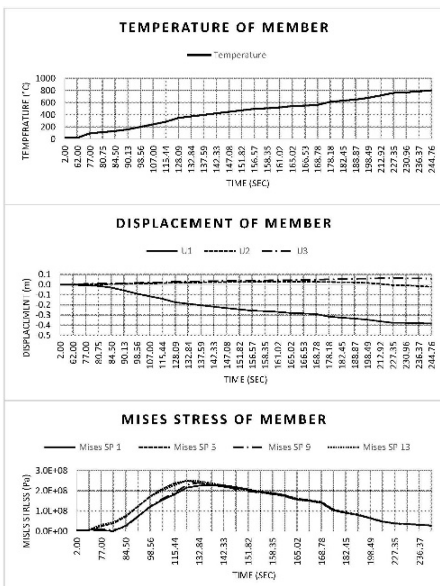

d) Case 2- Girt Node 481

Figure 11. Case 2 Results

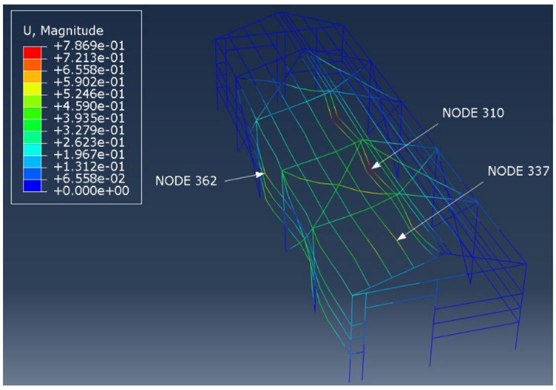

a) Case 3 Node Locations

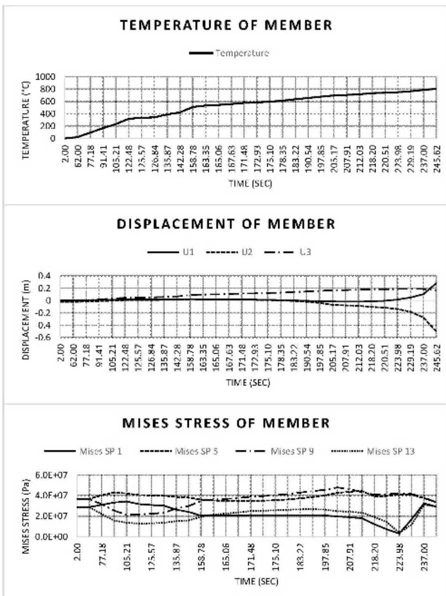

b) Case 3- Purlin Node 310

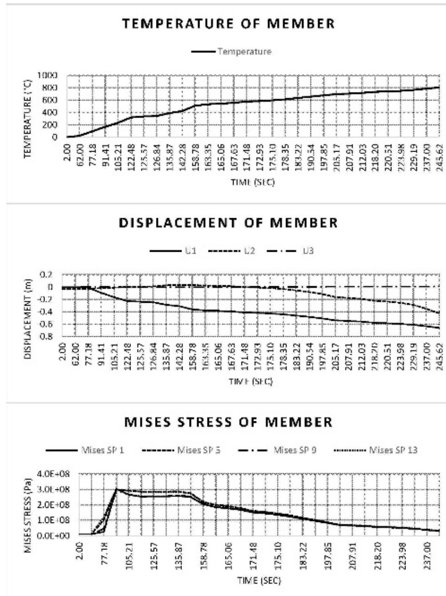

c) Case 3- Purlin Node 337

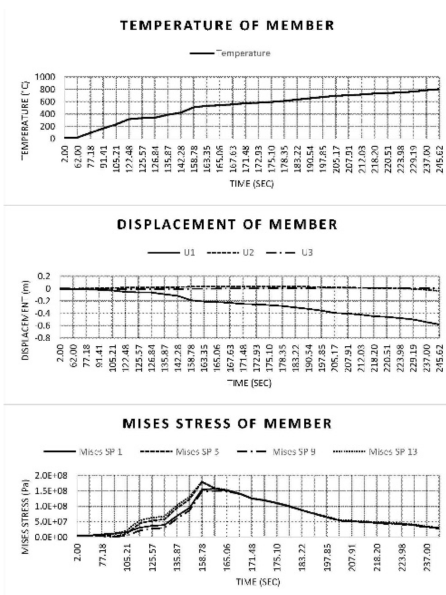

d) Case 3- Girt Node 362

Figure 12. Case 3 Results

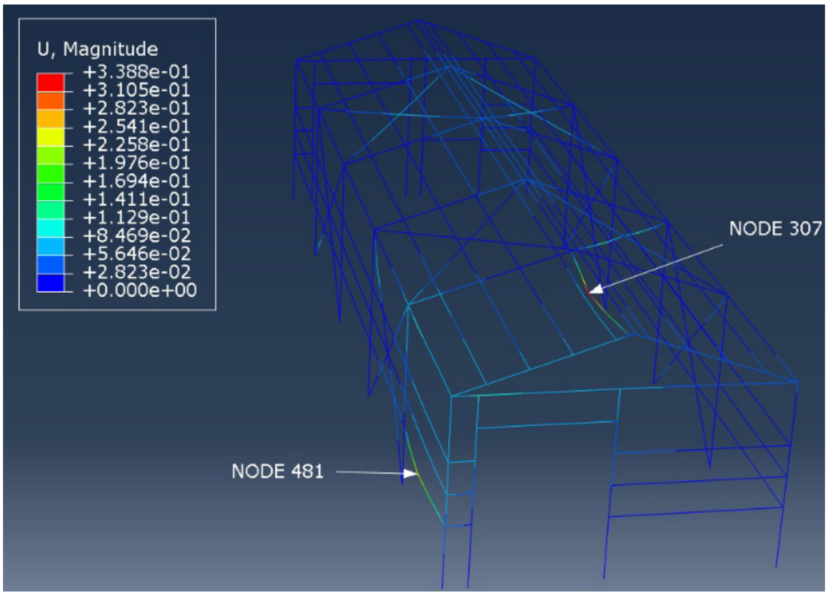

a) Case 4 Node Locations

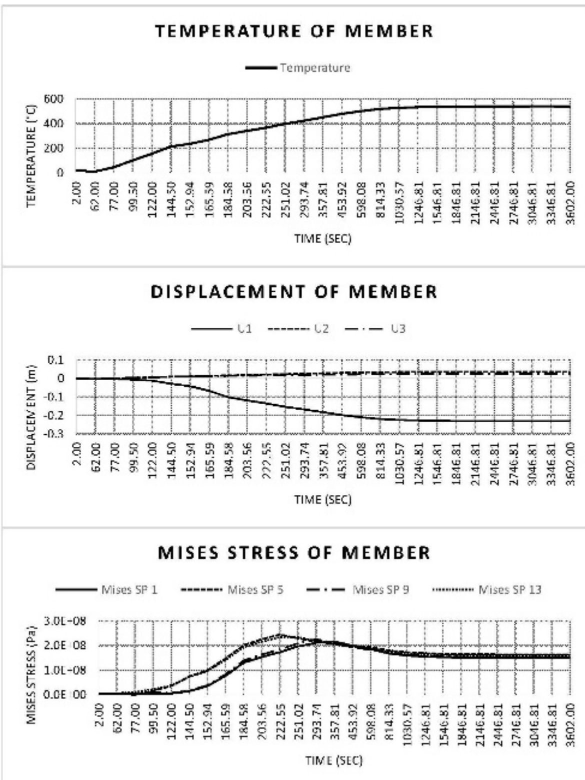

b) Case 4- Purlin Node 307

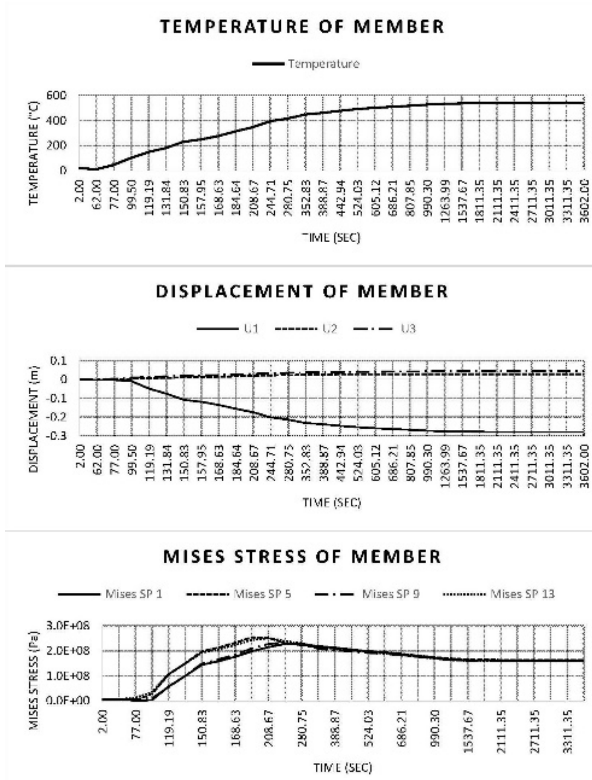

c) Case 4- Girt Node 481

Figure 13. Case 4 Results

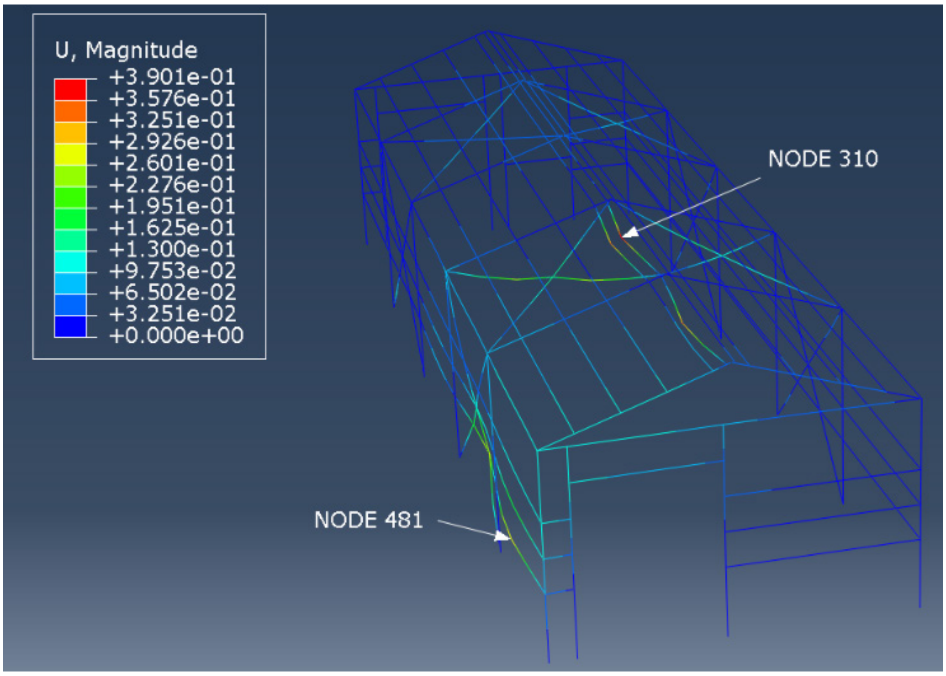

a) Case 5 Node Locations

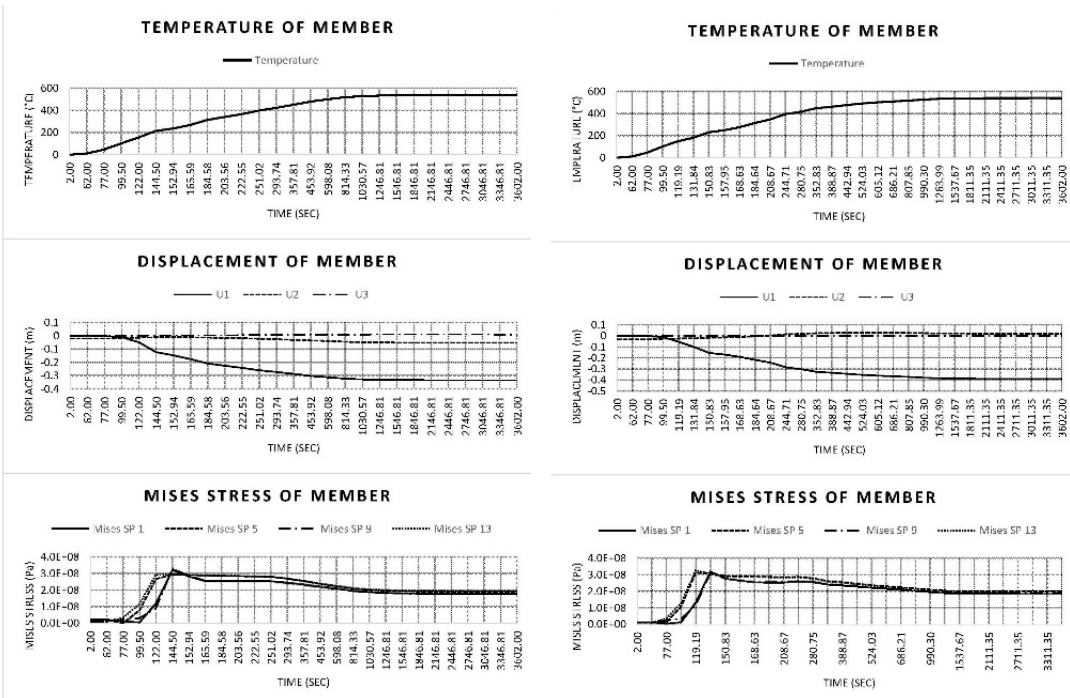

b) Case 5- Purlin Node 310 c) Case 5- Girt Node 481

Figure 14. Case 5 Results

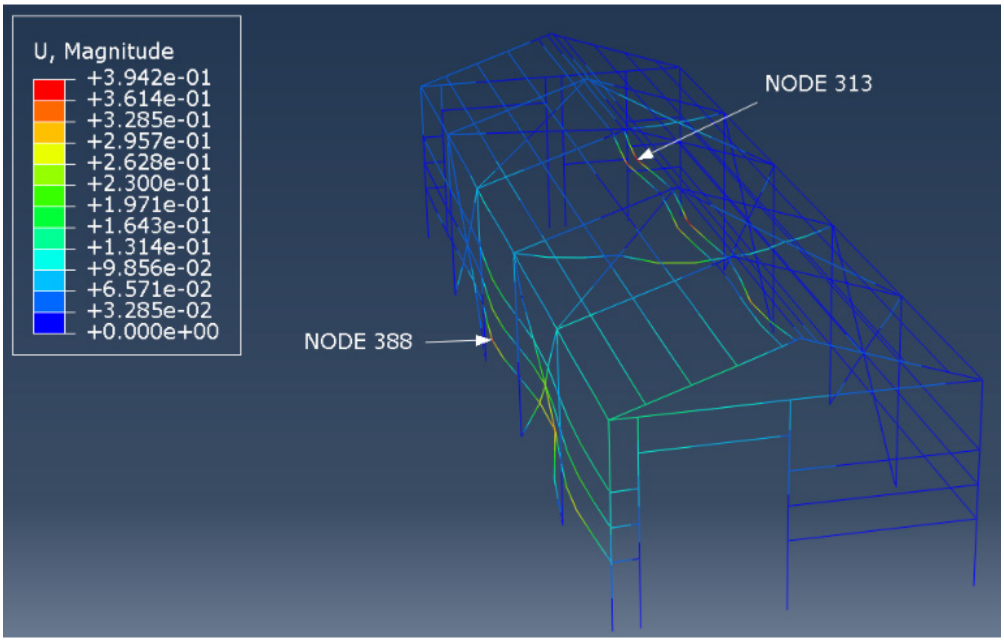

a) Case 6 Node Locations

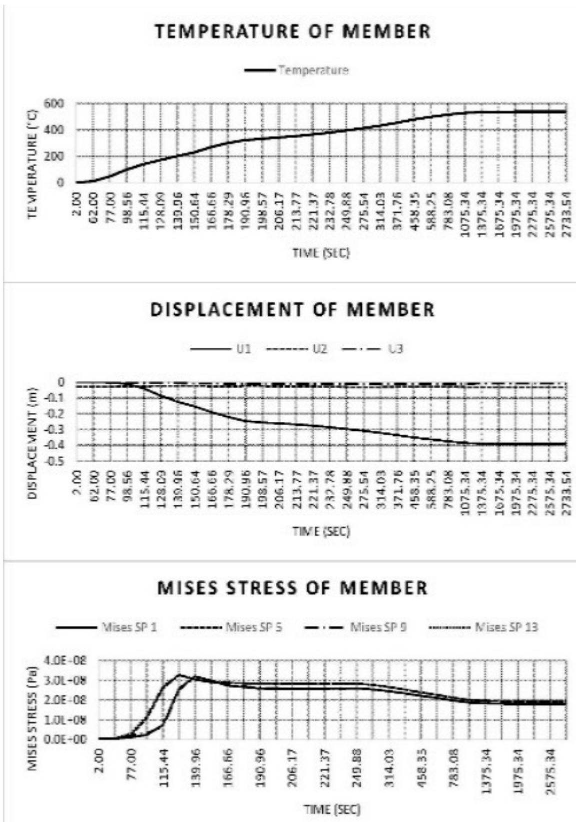

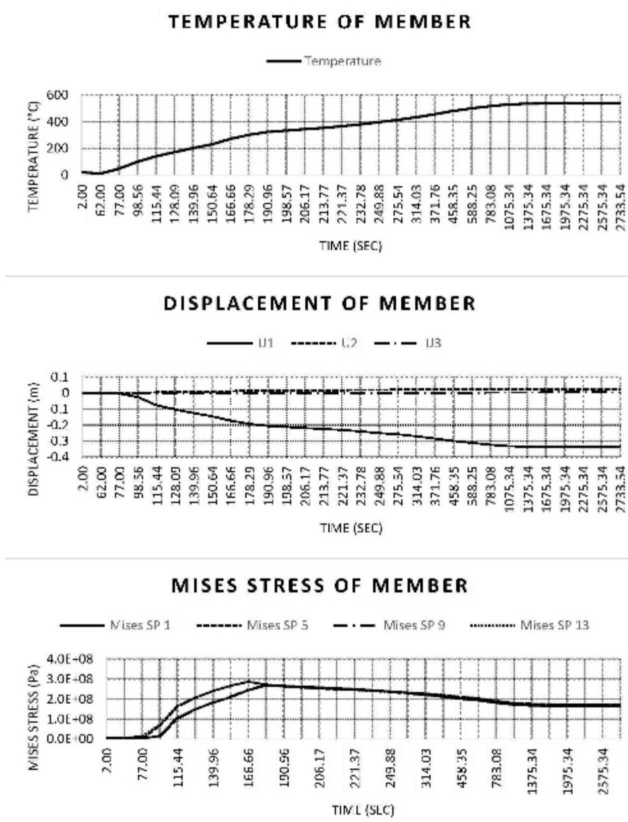

b) Case 6- Purlin Node 313 d) Case 6- Girt Node 388

Figure 15. Case 6 Results

Table 4. FEA Model – Maximum Temperature

Fire Protection	Bays Exposed to Fire	Case	Abaqus Model Run Time (sec)	Node Number	Member Type	Maximum Temperature			
						Time (sec)	Displacement (m)	Stress (pa)	Temperature (°C)
Unprotected	11	1	252.4	307	Purlin	252.4	0.4826	3.08E+07	814
				481	Girt	252.4	0.3503	2.90E+07	814
	11 and 12	2	244.8	325	Purlin	244.8	0.5967	3.40E+07	805
				340	Purlin	244.8	0.4552	3.26E+07	805
				481	Girt	244.8	0.3844	2.79E+07	805
	11, 12, and 13	3	245.6	310	Purlin	245.6	0.6614	3.31E+07	806
				337	Purlin	245.6	0.5044	3.34E+07	806
				362	Girt	245.6	0.5808	3.06E+07	806
Protected	11	4	3602	307	Purlin	3602	0.3345	1.95E+08	539
				481	Girt	3602	0.2309	1.64E+08	539
	11 and 12	5	3602	310	Purlin	3602	0.3896	1.99E+08	539
				481	Girt	3602	0.2799	1.64E+08	539
	11, 12, and 13	6	2733.5	313	Purlin	2733.5	0.3927	1.92E+08	539
				388	Girt	2733.5	0.3388	1.73E+08	539

Table 5. FEA Model – Maximum Stress

Fire Protection	Bays Exposed to Fire	Case	Abaqus Model Run Time (sec)	Node Number	Member Type	Maximum Stress			
						Time (sec)	Displacement (m)	Stress (pa)	Temperature (°C)
Unprotected	11	1	252.4	307	Purlin	92	0.0655	3.35E+08	168
				481	Girt	135.1	0.1468	2.42E+08	385
	11 and 12	2	244.8	325	Purlin	137.6	0.1857	2.67E+08	398
				340	Purlin	212.9	0.1216	3.70E+07	719
				481	Girt	128.1	0.1765	2.51E+08	348
	11, 12, and 13	3	245.6	310	Purlin	91.4	0.0925	3.04E+08	165
				337	Purlin	205.2	0.1675	4.78E+07	697
				362	Girt	158.8	0.1875	1.80E+08	510
Protected	11	4	3602	307	Purlin	144.5	0.1229	3.26E+08	213
				481	Girt	222.6	0.1353	2.45E+08	366
	11 and 12	5	3602	310	Purlin	119.2	0.0533	3.27E+08	148
				481	Girt	184.6	0.1569	2.54E+08	313
	11, 12, and 13	6	2733.5	313	Purlin	128.1	0.0865	3.28E+08	171
				388	Girt	166.7	0.1731	2.87E+08	270

Table 6. FEA Model – Maximum Absolute Displacement

Fire Protection	Bays Exposed to Fire	Case	Abaqus Model Run Time (sec)	Node Number	Member Type	Maximum Absolute Displacement			
						Time (sec)	Displacement (m)	Stress (pa)	Temperature (°C)
Unprotected	11	1	252.4	307	Purlin	252.4	0.4826	3.08E+07	814
				481	Girt	252.4	0.3503	2.90E+07	814
	11 and 12	2	244.8	325	Purlin	244.8	0.5967	3.40E+07	805
				340	Purlin	244.8	0.4552	3.26E+07	805
				481	Girt	244.8	0.3844	2.79E+07	805
	11, 12, and 13	3	245.6	310	Purlin	245.6	0.6614	3.31E+07	806
				337	Purlin	245.6	0.5044	3.34E+07	806
				362	Girt	245.6	0.5808	3.06E+07	806
Protected	11	4	3602	307	Purlin	3346.8	0.3345	1.95E+08	539
				481	Girt	3602	0.2309	1.64E+08	539
	11 and 12	5	3602	310	Purlin	3602	0.3896	1.99E+08	539
				481	Girt	3311.4	0.2799	1.64E+08	539
	11, 12, and 13	6	2733.5	313	Purlin	2733.5	0.3927	1.92E+08	539
				388	Girt	2733.5	0.3388	1.73E+08	539

Abaqus aborted analysis within the first four minutes for all three of the unprotected fire cases. Maximum deflections for the unprotected fire cases ranged from 330 mm (thirteen inches) to 661 mm (twenty-six inches). Abaqus also aborted analysis of Case 6, which is the protected fire case in which the three bays, Bays 11, 12, and 13, are exposed to the design fire curve, after nearly forty-six minutes. Although, maximum deflections for the Protected fire cases ranged from 228 mm (nine inches) to 406 mm (sixteen inches).

It is also observed that relatively large deformations occurred when more than two bays are exposed to a design fire such as case 3 where maximum displacement of 661 mm (twenty-six inches) occurred when three bays were on fire. This is also observed for case 6 when fire protection is utilized with maximum displacement is 392 mm (fifteen inches), therefore limiting the extent of the fire could be beneficial.

The three-dimensional modeling also helped in revealing interesting structural member interactions, which is shown in the different purlin and girder responses. This observation is lacking in the previous 2D models [25] and presents a more realistic failure response than from 2D modeling.

3.2 Limitations of Current Study

Current study did not include cases where battery fires reignite after the initial fire breakout and suppression, which has been documented to occur during several electric vehicle fires and prolonged the efforts to put out the fires [31]. While this did not occur for the Houston train fire case, the risk can be very high for large containers of wasted Li-ion batteries. How to establish a prolonged and multi-staged fire curve for battery fire is a critical information necessary for structure fire analysis.

Current study uses a hydrocarbon fire to simulate the propagation of a LIB fire, which does not include the explosive nature of a large pack lithium ion battery fire, similar to the Houston fire of the train carrying large amount of waste batteries. Currently, there is no large-scale LIB fire studies and hence, is a very critical limitation. The research team is working towards establishing experimental battery fire time histories that will be applied to the 3D structural models.

There is a quadruple increase in LIB applications, especially in large-scale utilities such as energy storages. Correspondingly, there is an increase in LIB fires, which further demonstrated the importance of such studies as demonstrated in this paper. As trains are a very likely means of transport for waste batteries, there is an urgent need to investigate LIB fires to neighboring structures. The analysis process demonstrated in current paper represent a critical first step towards the understanding of large-scale LIB fires and can be a useful approach for future fire risk evaluation of any structure types.

4. Conclusions

LIB fire due to depleted battery stockpiles has drawn critical attentions during the 2017 Houston train fire incidence. Even though fire regulations are not addressing the fire safety issues of waste LIB transportation yet, there is a need to establish a holistic approach to evaluate fire risk potentials. This paper investigated the fire risks of a steel frame structure using 3D FE modeling. The 3D analysis allowed us to visualize the selected fire scenario and helped identify the most critical members subject to battery fire and their performances. The fire study was based on the North Carolina Capital Railyard Warehouse with multiple potential train access sites.

When considering the fire safety and control of a fire, the most significant fire scenario was determined to be a battery train fire within the warehouse which could potentially be caused by thermal runaway and is more difficult to control than a conventional fire.

Based on the assumptions made and data available from the 3D finite element model, it appears that structural components would experience relatively large stresses and deflections during a design fire and the structure could potentially become unstable. The analysis appears to demonstrate that utilizing fire protection could slow the rate at which structural steel members would deflect, reduce the total deflection experienced by a structural member, and delay or prevent structural instability. The research also indicates that structural instability could occur if more than two bays are exposed to a design fire even if fire protection is utilized, therefore limiting the extent of the fire could be beneficial.

Finally, the 3D modeling reveals interesting and more realistic member interactions during the fire propagation than two-dimensional modeling.

Acknowledgements

The authors would like to extend their thanks and acknowledge the North Carolina Department of Transportation (NCDOT) for the data they provided and their collaboration. Any opinions, findings, and conclusions expressed in this paper are those of the authors and do not necessarily reflect the views of the NCDOT. The research team would like to acknowledge technical contributions from Jasmine Mira and 2020 spring senior design team members: Peter Theilgard, Marwa Elkazzaz, Seth Cathey and David Vences.

Conflict of Interest

There is no conflict of interest.

References

[1] Armand, M., Axmann, P., Bresser, D., et al., 2020. Lithium-ion Batteries- Current State of the Art and Anticipated Developments, Journal of Power Sources. 479, 228708.

[2] Notter, D.A., Gauch, M., Widmer, R., et al., 2010. Contribution of Li-ion batteries to the Environmental Impact of Electric Vehicles. Environmental Science Technologies. 44, 6550-6556.

[3] Church, C., Wuennenberg, L., 2019. Sustainability and Second Life: The Case for Cobalt and Lithium Recycling, Technical Report, International Institute for Sustainable Development (IISD). pp. 68.

[4] Federal Register, 2007. Hazardous Materials; Transportation of Lithium Batteries. 49 CFR Parts 171, 172, 173 and 175, Pipeline and Hazardous Materials Safety Administration (PHMSA), USDOT.

[5] Houston Fire Department, 2017. "Chapman Street Fire," Report No. 17-1120608, Houston Fire Department.

[6] Romo, S.N., 2020. Personal Communication, KTRK-TV.

[7] Summer, S., Maloney, T., 2017. Fire Hazard Analysis for Various Lithium Batteries, Report No. DOT/FAA/TC-16/17, US Department of Transportation.

[8] Wang, Q., Ping, P., Zhao, X., et al., 2012. Thermal Runaway Caused Fire and Explosion of Lithium Ion Battery. Journal of Power Sources. 208, 210-224.

[9] Long, Jr.R.T., Sutula, J.A., Kahn, M.J., 2014. Flammability of Cartoned Lithium Ion Batteries, the Fire Protection Research Foundation, Springer, New York.

[10] Larsson, F., Anderson, J., Andersson, P., et al., 2016. Thermal Modelling of Cell-to-Cell Fire Propagation and Cascading Thermal Runaway Failure Effects for Lithium-Ion Battery Cells and Modules Using Fire Walls. Journal of Electrochemical Society. 163(14), A2854-A2865.

[11] Blum, A.F., Long, Jr.R.T., 2016. Fire Hazard Assessment of Lithium Ion Battery Energy Storage Systems, Springer, New York.

[12] DNV-GL, 2020. McMicken Battery Energy Storage System Event Technical Analysis and Recommendations. Arizona Public Services Report No. 10209302-HOU-R-01.

[13] APTA, 2009. Recommended practice for Transit Bus Fire/Thermal Incident Investigation, APTA BTS-BS-RP-004-08.

[14] APTA, 2009. Recommended practice for Transit Bus Electrical System Requirements Related to Fire Safe-

ty, APTA BTS-BS-RP-002-07.

[15] APTA, 2009. Recommended Practice for Installation of Transit Vehicle Fire Protection Systems, APTA BTS-BS-RP-003-08.

[16] APTA, 2009. Recommended practice for Fire Safety Analysis of Existing Passenger Rail Equipment, APTA BTS-BS-RP-005-00.

[17] APTA, 2009. Recommended practice for Fire Detection System Inspection and Testing, APTA RT-SC-S-042-03.

[18] NFPA, Standard for Fixed Guideway Transit and Passenger Rail Systems, NFPA-130, National Fire Protection Association, Washington, D.C, 2020.

[19] IBC (International Building Code), 2018. International Code Council, Washington, D.C.

[20] LaMalva, K., 2018. Structural Fire Engineering, ASC/SEI Manual of Practice.

[21] MBMA, 2010. Fire Resistance Design Guide for Metal Buildings Systems, Manual, Metal Building Manufacturers Association, Ohio.

[22] MBMA, 2018. Metal Building Systems Manual, Handbook. Metal Building Manufacturers Association, Ohio.

[23] MBMA, 2018. Seismic Design Guide for Metal Building Systems, Metal Building Manufacturers Association, Third Edition, Ohio.

[24] AISC (American Institute of Steel Construction), 2017. Steel Construction Manual, 15th Edition. Chicago.

[25] Mira, J., Braxtan, N.L., Chen, S.E., et al., 2021. Battery Train Fire Risk on a Steel Warehouse Structure. Journal of Architectural Environment and Structural Engineering Research. 4, 3.

[26] Abaqus, 2018. User's Manual, Abaqus Inc., Johnston, RI.

[27] Haehler, R., 2011. Steel Design Guide 25: Frame Design Using Web-Tapered Members. Steel Design Guide Series Number 25, AISC.

[28] ASCE/SEI, 2016. American Society of Civil Engineers, ASCE Standard 7-16 Minimum Design Loads and Associated Criteria for Buildings and Other Structures. Virginia.

[29] EN 1993-1-1, 2005. Eurocode 3: Design of Steel Structures - Part 1-2: General rules – Structural Fire Design. Brussels: Comité Européen de Normalisation.

[30] EN 1991-1-2, 2009. Eurocode 1: Actions on Structures - Part 1-2: General Actions - Actions on Structures Exposed to Fire. Brussels: Comité Européen de Normalisation.

[31] Sun, P., Huang, X., Bisschop, R., et al., 2020. A Review of Battery Fires in Electric Vehicles. Fire Technology. 56, 1361-1410.

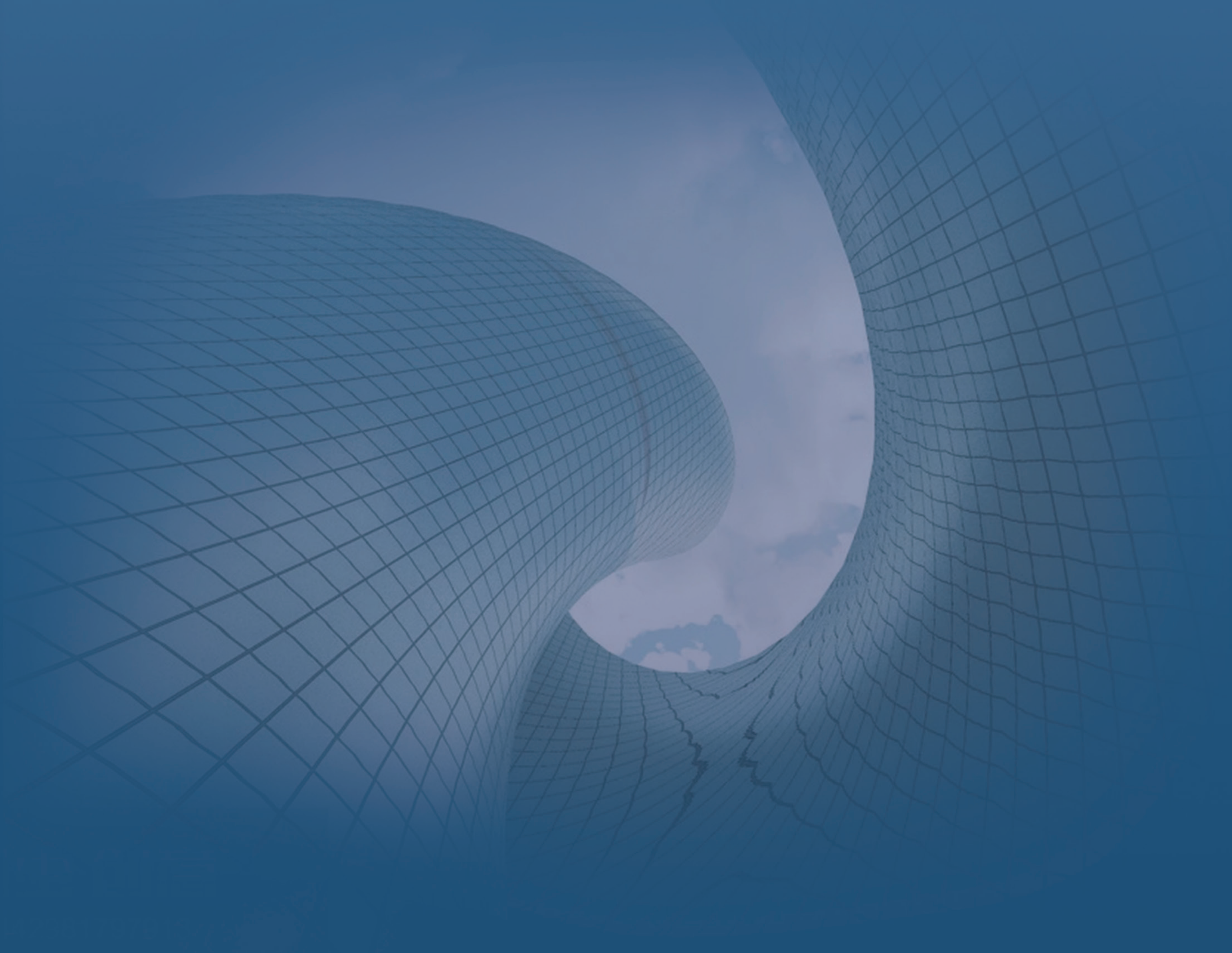

BILINGUAL PUBLISHING CO.
Pioneer of Global Academics Since 1984

Tel.:+65 65881289
E-mail: contact@bilpublishing.com
Website:ojs.bilpublishing.com

2630-5232
03